ISSN 1023-9855

Thoracic Medicine

Volume 37 • Number 1 • March 2022

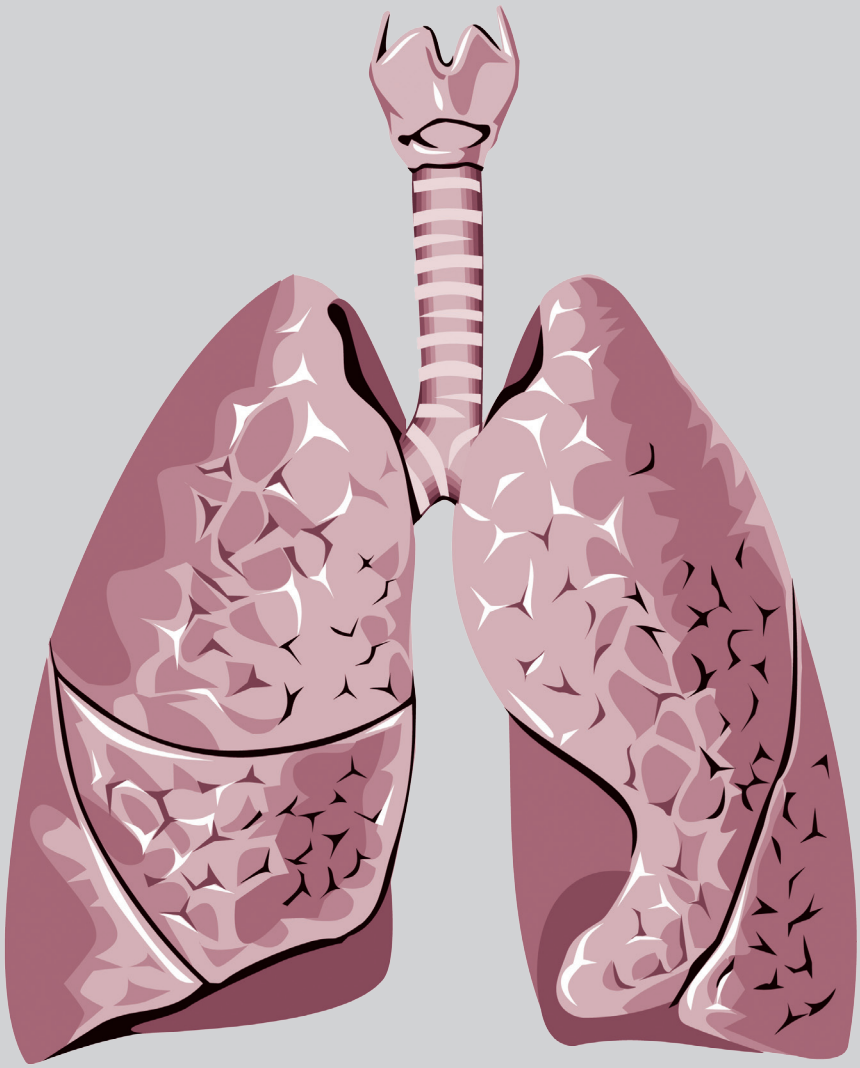

The Official Journal of

Taiwan Society of Pulmonary and Critical Care Medicine

Taiwan Society of Sleep Medicine

Taiwan Society for Respiratory Therapy

Taiwan Society of Tuberculosis and Lung Diseases

Thoracic Medicine

The Official Journal of
Taiwan Society of Pulmonary and Critical Care Medicine
Taiwan Society for Respiratory Therapy
Taiwan Society of Sleep Medicine
Taiwan Society of Tuberculosis and Lung Diseases

Thoracic Medicine

The Official Journal of
Taiwan Society of Pulmonary and Critical Care Medicine
Taiwan Society for Respiratory Therapy
Taiwan Society of Sleep Medicine
Taiwan Society of Tuberculosis and Lung Diseases

Volume 37
Number 1
March 2022

CONTENTS

Long-Acting Beta-2 Agonist and Theophylline Attenuate Cigarette Smoke-Induced Airway Inflammation through Regulation of Cyclic Adenosine Monophosphate

Yu-Jung Lin[1], Kang-Cheng Su[2,3,4], Yi-Han Hsiao[3,4,5]

Introduction: Adding theophylline, a non-selective phosphodiesterase (PDE) inhibitor, to a long-acting beta-2 agonist (LABA) provides an additive bronchodilation effect through preventing cyclic adenosine monophosphate (cAMP) degradation. This procedure has become a common therapeutic choice in the management of chronic obstructive pulmonary disease patients. Emerging studies have shown that the use of a LABA and PDE inhibitor may inhibit airway inflammation, but details of the mechanism require further investigation.

Methods: Mice were exposed to cigarette smoke (CS) for 4 weeks to induce airway inflammation. Indacaterol maleate (IND, a LABA), theophylline, and their combination or a vehicle was given through intraperitoneal injection daily during the 4-week exposure. In addition, human primary bronchial epithelial cells (PBECs) were exposed to cigarette smoke extract (CSE) with or without treatment of IND or theophylline. Interleukin (IL)-8 production and the cAMP level in PBECs were measured. Inhibitors of downstream signaling, including adenylyl cyclase (AC) and protein kinase A (PKA), were used to evaluate the underlying mechanism.

Results: IND, theophylline and their combination reduced CS-induced protein leakage and inflammatory cells accumulation in the bronchoalveolar lavage fluid, as well as lung inflammation and peribronchial collagen deposition in lung sections. IND and theophylline consistently inhibited CSE-induced increases in IL-8 production in PBECs through maintaining the cAMP level. This anti-inflammatory effect was alleviated by adding AC or PKA inhibitor.

Conclusion: Both LABA and theophylline exert a potent inhibitory effect on CS-induced airway inflammation through regulating cAMP and the AC-PKA pathway. ***(Thorac Med 2022; 37: 1-12)***

Key words: long-acting beta-2 antagonist, phosphodiesterase inhibitor, airway inflammation

[1]Department of Chest Medicine, Taipei Veterans General Hospital, Taipei, Taiwan, [2]Division of Clinical Respiratory Physiology, Department of Chest Medicine, Taipei Veterans General Hospital, Taipei, Taiwan, [3]Department of Physiology, School of Medicine, National Yang Ming Chiao Tung University, Taipei, Taiwan, [4]Faculty of Medicine, School of Medicine, National Yang Ming Chiao Tung University, Taipei, Taiwan, [5]Division of General Chest Medicine, Department of Chest Medicine, Taipei Veterans General Hospital, Taipei, Taiwan.
Address reprint requests to: Dr. Yi-Han Hsiao, Division of General Chest Medicine, Department of Chest Medicine, Taipei Veterans General Hospital, 201 Shih-Pai Road, Section 2, Taipei 11217, Taiwan

Introduction

Chronic obstructive pulmonary disease (COPD) is a global health issue, with cigarette smoking (CS) being one of the most important risk factors [1]. Inhaled CS causes chronic lung inflammation and damage through affecting the repair function of many types of pulmonary cells [2], followed by inadequate control of fibroblast repair, causing airway remodeling. For example, airway epithelial cells, which are located in the most superficial layer of the airways, are first exposed and activated by CS, and then not only release chemotactic factors that attract inflammatory cells to the lungs [3-4], but also release transforming growth factor-β (TGF-β), which stimulates fibroblast proliferation, resulting in fibrosis in the small airways [5]. Various cells and mediators are involved in this inflammatory process, but the detailed underlying mechanism is still largely unexplored.

Progression of COPD is associated with the accumulation of inflammatory cells [6], and exacerbation of COPD is linked to additional increases in airway inflammation mediated by neutrophils, lymphocytes, eosinophils, and interleukin (IL)-8 [7]. A medication that can reduce exacerbation may indicate its anti-inflammatory effect. Long-acting beta-2 agonist (LABA), which upregulates intracellular cyclic adenosine monophosphate (cAMP), is a principal bronchodilator in the treatment of COPD. Indacaterol (IND), the first once-daily LABA approved for treatment of COPD, not only improves pulmonary function, but also reduces acute exacerbation of COPD [8-9]. An exchange protein directly activated by cAMP and protein kinase A (PKA) can decrease cigarette smoke extract (CSE)-induced IL-8 released by human airway smooth muscle cells via inhibition of the nuclear factor kappa-light-chain-enhancer of activated B cells (NF-κB) and extracellular signal-regulated protein kinase (ERK), respectively, indicating these cAMP effectors as potential targets for anti-inflammatory therapy in COPD [10]. Nevertheless, LABA alone seems not the optimal treatment for COPD in the current guideline [11], suggesting the emerging need of combination therapy.

Phosphodiesterase (PDE) inhibitor prevents cAMP degradation and provides LABA with an adjunctive bronchodilator effect. Selective PDE4 inhibitors, especially, offered a benefit over placebo in reducing exacerbation of COPD [12], as well as the number of inflammatory cells in induced sputum samples of patients with COPD [13]. However, the small clinical improvement with roflumilast, its gastrointestinal adverse effects and its cost prevent it from becoming a first-line medication, and it is suggested only for severe, uncontrolled COPD, despite its use as inhaled therapy in the latest guideline [11]. Theophylline (TH), a non-selective PDE inhibitor developed earlier and more widely used in airway diseases, showed its ability to inhibit fibroblast proliferation and TGF-β-induced alpha-SMA protein via the cAMP-PKA pathway [14]. However, whether TH can provide an additive effect to LABA in inhibiting CS-induced airway inflammation through the cAMP-PKA pathway remains unknown. Therefore, the aim of our study was to investigate this hypothesis in a CS-exposed mouse model and in an *in vitro* model using primary bronchial epithelial cells (PBECs).

Materials and Methods

Ethics statement

All animal experiments were approved by the Animal Care and Use Committee of National Yang-Ming University. Human PBECs were obtained from lung cancer patients who underwent surgical lobectomy. This study was approved by the Institutional Review Board of Taipei Veterans General Hospital (IRB-TPEVGH No.: 2015-06-005A and 2015-10-004A).

Murine model of chronic CS exposure

The murine model of chronic CS exposure has been described in detail previously [3]. Male C57BL/6J mice at 8 weeks of age (National Laboratory Animal Center, Taipei, Taiwan) were randomly divided into 6 groups (n=5 mice/group) for a 4-week exposure to CS or air. Two of the CS-exposure groups received daily treatment with IND (Novartis® Pharmaceuticals, Taiwan; 5 μg/kg) or TH (Sigma-Aldrich, St. Louis, MO, USA; 10 mg/kg) [15] or a saline vehicle at the same volume (60 μL) by intraperitoneal injection during the 4-week exposure. The intraperitoneal route of drug administration provides rapid and efficient absorption with a low level of stress in laboratory rodents and is considered as an adequate route for pharmacological and proof-of-concept studies [16]. Thus, the mice were formed into 6 groups, namely Air, CS, CS+normal saline (NS), CS+IND, CS+TH, and CS+IND+TH. The animals were given ad libitum access to food and water, and the average body weight among the study groups did not vary after a 4-week exposure. For each CS exposure, the mice were placed in an exposure chamber and 750 ml of fresh CS generated from 1.5 cigarettes (Marlboro Red Label; 10.8 mg nicotine and 10.0 mg tar per cigarette) was delivered into the chamber. The CS passed out of the chamber via 4 exhaust holes (1 cm) on the side panels. During the exposure, the mice were conscious and breathed spontaneously in the chamber for 10 min. After exposure, the mice were transferred to a new cage and allowed to inspire air normally. The mice were exposed at 10:00 and 16:00 each day for 4 weeks. The control animals underwent identical procedures in another chamber but were only exposed to air. For each CS exposure, the particle concentration inside the exposure chamber was about 625 mg/m^3 initially, but decreased over time since the CS passed out of the chamber via the exhaust holes [3]. The HbCO levels immediately after the 10-minute exposure protocol for the air-exposed and CS-exposed mice were 0.4% and 32%, respectively [3].

Preparation of bronchoalveolar lavage fluid (BALF) and lung tissues

At the end of each experiment, the mice were euthanized with carbon dioxide (CO_2) and a middle thoracotomy was performed. The left lung was ligated, and the right lung was lavaged 4 times with warm PBS (0.6 ml) containing a complete protease inhibitor cocktail (Roche Diagnostics, Mannheim, Germany). The samples of BALF were centrifuged at 350 g for 5 min at 4°C, and the supernatant of the first lavage fluid was stored at −80°C for later analysis of total protein using a Bio-Rad protein assay reagent (Bio-Rad Laboratories, Inc., Hercules, CA, USA). The cell pellets of the BALF samples were resuspended in PBS for cell counting. The right lung was then stored at -80°C for subsequent analysis. The left lung was fixed with 4% paraformaldehyde and embedded in paraffin.

Histological assessment

Formalin-fixed, paraffin-embedded tissue blocks were cut into 8-μm sections. Sections

were deparaffinized, rehydrated, and then covered with 3% H_2O_2 for 10 min. The slides were counterstained with hematoxylin and eosin (H&E) for cellular infiltration and Masson's trichrome for peribronchial collagen deposition.

Experimental protocols for in vitro studies

PBECs were seeded onto 24-well culture inserts and grown in culture medium. Cells were stimulated by CS extract (CSE, 3%) [3] for the desired length of time. To suppress the CSE-induced responses, cells were pretreated with a vehicle, IND (100 nM) or TH (100 nM), for 2 hours before changing to fresh medium and stimulation. Supernatants were collected for assay of cAMP and IL-8 using an ELISA kit (R&D Systems, Minneapolis, MN, USA) after stimulation for 24 hours, according to the manufacturer's instructions. Inhibitors of AC (KH7; 25 μM; R&D Systems, Minneapolis, MN, USA) [17] or PKA (H89; 10 μM; Sigma Aldrich, St. Louis, MO, USA) [18] were added with IND or TH for 2 hours before changing to fresh medium and stimulation. Cell viability was determined by light microscopy and dye exclusion with trypan blue. In these experiments, the concentrations of CSE, IND, TH, KH7 and H89, and the optimal time point for the measurements of the responses were obtained from our previous investigations or preliminary study.

Modified air-liquid interface culture for PBECs

Preparation of the modified air-liquid interface culture for PBECs has been described in detail previously [3, 19]. Human bronchus, obtained from a non-tumor part of surgical specimens from patients who received lobectomy for lung cancer, was rinsed several times with Leibovitz's L-15 medium containing penicillin (100 U/ml), streptomycin (100 μg/ml), and amphotericin B (0.25 μg/ml). The tissue was cut into 1-2 mm^2 pieces and 3 to 4 pieces of tissue were planted with the epithelium side facing down onto 6-well culture inserts (growth area of the membrane: 4.2 cm^2, pore size: 0.4 μm) coated with type IV collagen (50 μg/cm^2). Two ml of PBEC culture medium, containing antibiotics/antimycotic, insulin (2.5 μg/ml), transferrin (2.5 μg/ml), hydrocortisone (1 μg/ml), glutamine (2 mM), and 0.1% FBS in RPMI 1640 and Medium 199 (v/v 1:1), was added to the basal chamber, and 100 μl was added to the insert. Culture medium in the basal chamber was changed every 48 to 72 hours, and no medium was added to the insert. PBECs were grown on a porous membrane, on which they formed a continuous epithelial sheet with the basal aspect exposed to the medium and the apical surface exposed to air.

Preparation of CSE

CSE was freshly prepared on the day of the experiment, as described [20, 21], with some modifications. Briefly, 1000 ml of smoke generated from 2 combusted cigarettes (Marlboro Red Label; tar, 10.0 mg; nicotine, 0.8 mg; size, 84 mm) without filters was sucked at a constant flow rate (8 ml/s) into a syringe and then bubbled into a tube containing 20 ml serum-free medium. The CSE solution was sterilized through a 0.22-μm filter (Millipore, Bedford, MA, USA) and its pH was adjusted to 7.4. The optical density of the CSE solution was checked by measuring the absorbance at 302 nm to reflect the level of peroxynitrite [22], which showed little difference between different preparations. This CSE solution was considered 100% CSE and was further diluted by serum-

free medium to the desired concentrations to stimulate cells at different time points.

Statistical analysis

Data are expressed as mean ± standard error of the mean (SEM). The comparison between different experimental conditions was evaluated by analysis of variance (ANOVA) followed by the least significant difference (LSD) test, when appropriate. A p value < 0.05 was considered significant.

Results

Suppressive effects of IND and TH on CS-induced lung inflammation in mice

Exposure of mice to CS for 4 weeks resulted in the development of lung inflammation. Relative to the air-exposed mice, the CS-exposed mice were found to show increases in total cell counts (Fig. 1A), total protein levels (Fig. 1B), and differential cell counts, including macrophages (Fig. 2A), neutrophils (Fig. 2B),

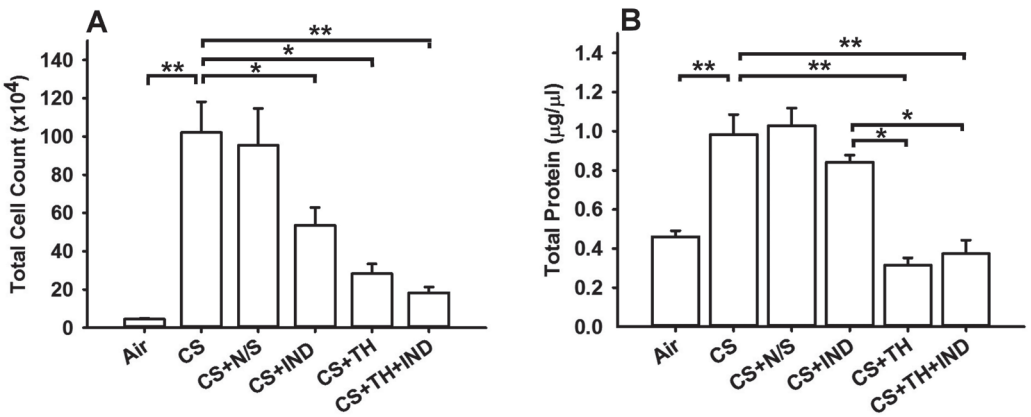

Fig. 1. Treatment with indacaterol maleate (IND, a long-acting beta-2 agonist), theophylline (TH, a phosphodiesterase inhibitor) or their combination alleviated cigarette smoke (CS)-induced increases in (A) total cell count and (B) total protein level in bronchoalveolar lavage fluid (BALF) sampled from mice. Mice were exposed to air or CS for 4 weeks with or without daily treatment intraperitoneally with saline (N/S; vehicle), IND (5 μg/kg), TH (10 mg/kg) or a combination of IND and TH. Data in each group are mean ± SEM from 4-5 mice. *, $p < 0.05$; **, $p < 0.01$.

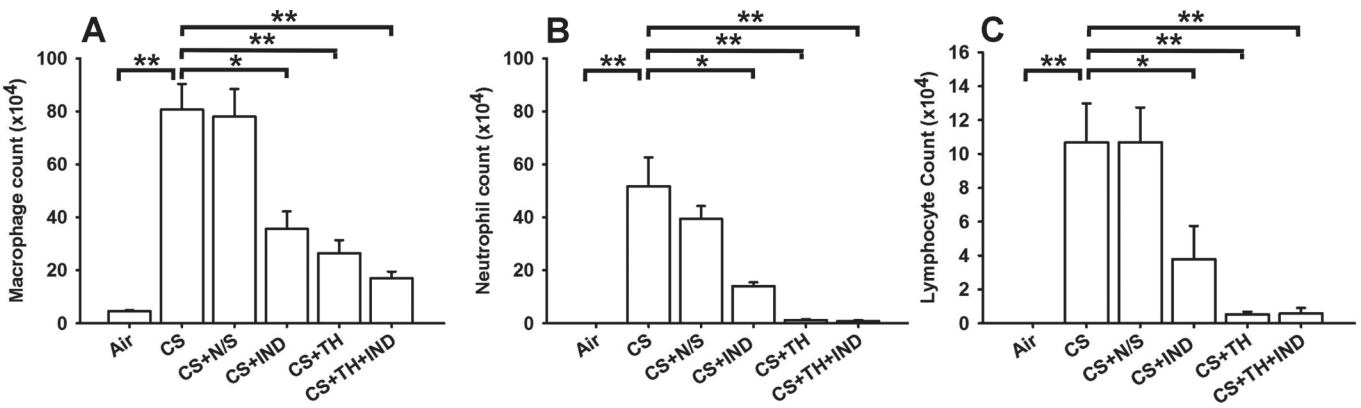

Fig. 2. Treatment with indacaterol maleate (IND, a long-acting beta-2 agonist), theophylline (TH, a phosphodiesterase inhibitor), or their combination alleviated cigarette smoke (CS)-induced increases in (A) macrophage, (B) neutrophil, and (C) lymphocyte counts in bronchoalveolar lavage fluid (BALF) sampled from mice. Mice were exposed to air or CS for 4 weeks with or without daily treatment intraperitoneally with saline (N/S; vehicle), IND (5 μg/kg), TH (10 mg/kg) or a combination of IND and TH. Data in each group are mean ± SEM from 4-5 mice. *, $p < 0.05$; **, $p < 0.01$.

and lymphocytes (Fig. 2C) in BALF. Treatment with IND, TH, or their combination, but not saline treatment, significantly reduced these inflammatory indices in CS-exposed mice (Figs. 1, 2). In addition, a histological evaluation of the H&E-stained lung sections (Fig. 3A) revealed extensive infiltration of inflammatory cells and thickening of the alveolar walls in the CS-exposed mice. The Masson's trichrome-stained lung sections (Fig. 3B) showed increased collagen (blue-stained) deposition at the peribronchial area. The differences in the degree of histopathological manifestations between groups was confirmed by comparing quantitative data from the 6 study groups in terms of lung inflammatory scores [23] (Fig. S1A) and the peribronchial collagen area [3] (Fig. S1B). Of note, all of these histopathological signs of inflammation were found to not be influenced by daily saline treatment, but there were fewer

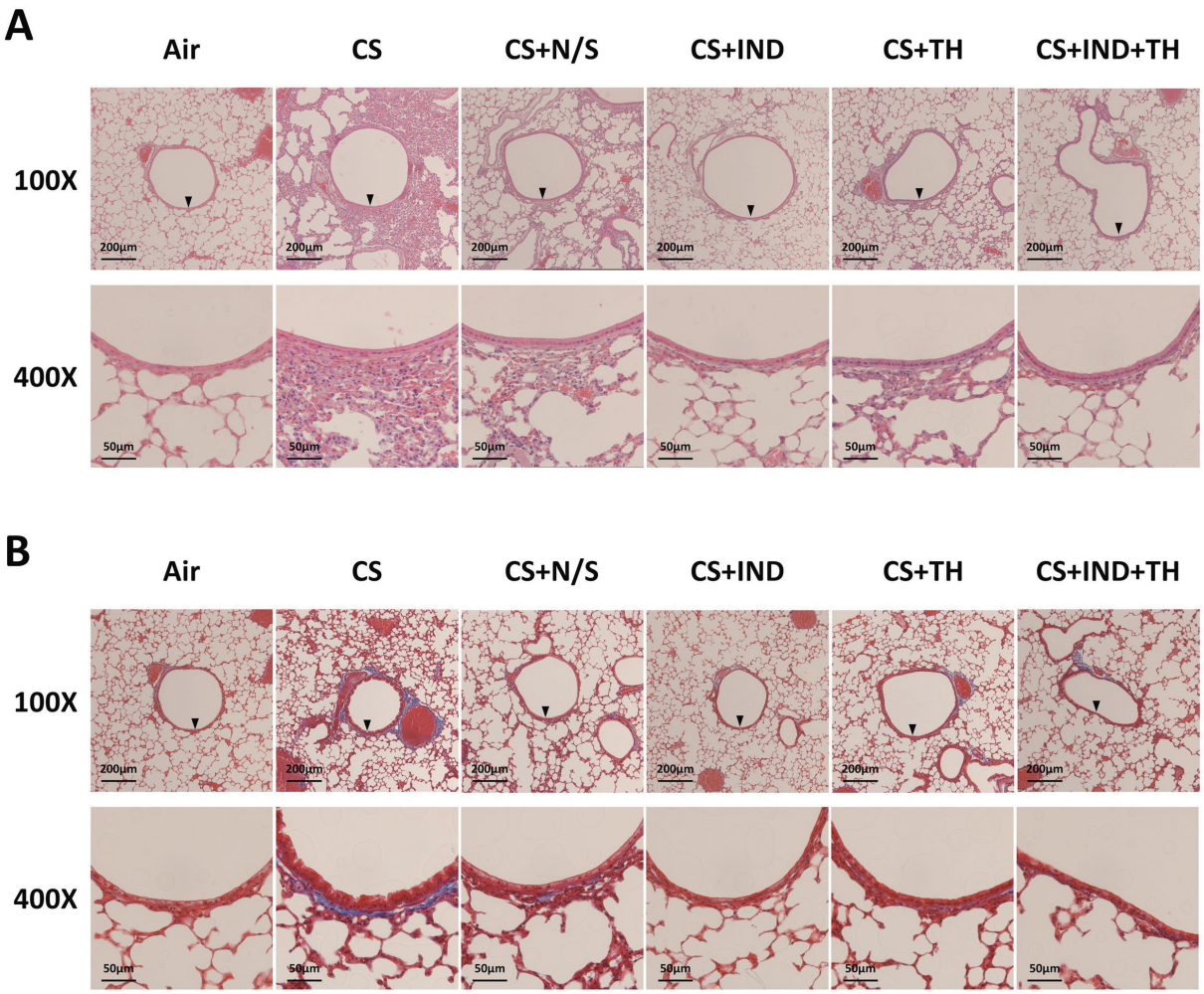

Fig. 3. Representative images of (A) H&E- and (B) Masson's trichrome-stained lung sections obtained from mice from 6 study groups. Mice were exposed to air or cigarette smoke (CS) for 4 weeks with or without daily treatment intraperitoneally with saline (N/S; vehicle), indacaterol maleate (IND, 5 μg/kg), theophylline (TH, 10 mg/kg) or a combination of IND and TH. The magnifications are 100X and 400X for the upper and lower panels, respectively. Arrows indicate the positions for large magnification (400) shown in lower panels. Note that CS exposure produced extensive infiltration of inflammatory cells and increased peribronchial collagen (blue-stained) deposition, which showed no significant difference in saline-treated mice. In contrast, treatment with IND, TH, or their combination markedly alleviated these signs of inflammation.

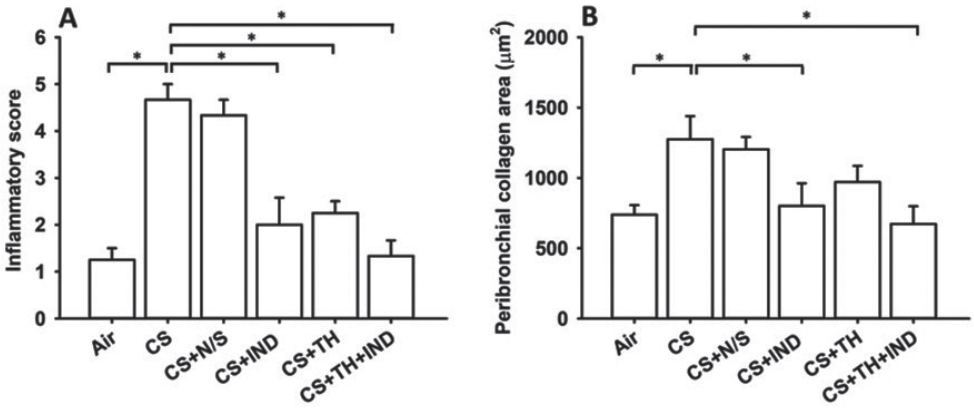

Fig. S1. Treatment with IND, TH or IND+TH alleviated elevations in (A) the inflammatory score and (B) peribronchial collagen deposition in the lungs of cigarette smoke (CS)-exposed mice. Mice were exposed to air or CS for 4 weeks with or without daily treatment intraperitoneally with saline (NS; vehicle), IND (5 μg/kg), TH (10 mg/kg) or a combination of IND and TH. The grade of lung inflammation was scored on a scale of 0–5. Lung inflammatory scores were calculated according to the sum of the levels of cell infiltration and peribronchial cuffing assessed by a pathologist who was blinded to the experiment. Peribronchial collagen areas were directly measured using Motic Images Plus 2.0. Data in each group are mean ± SEM from 4-5 mice. *, $p < 0.01$.

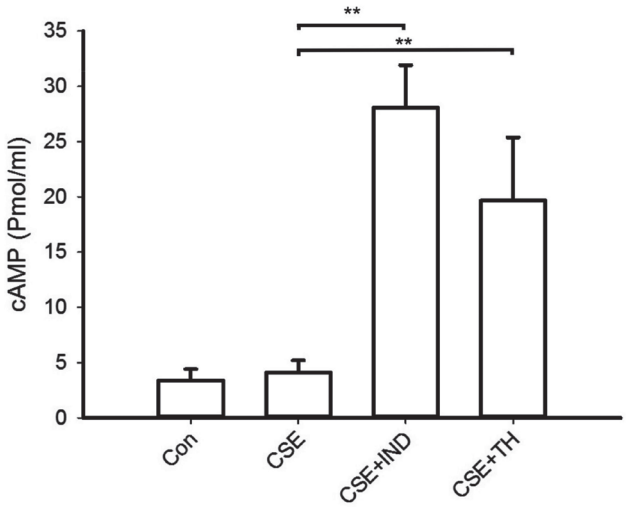

Fig. 4. Treatment with indacaterol maleate (IND) or theophylline (TH) increased the cyclic AMP (cAMP) level in primary bronchial epithelial cells (PBECs) after stimulation with cigarette smoke extract (CSE). Cells were exposed to 3% CSE with pretreatment with a vehicle, IND (100 nM) or TH (100 nM). Control groups (Con) were cells without stimulation and pretreatment. cAMP levels in cell lysates were analyzed by ELISA assay. Data in each group are mean ± SEM from 3-4 independent experiments. **, $p < 0.01$.

in the CS-exposed mice that underwent treatment with IND, TH, or their combination.

Effects of IND or TH on CSE-stimulated PBECs

In our in vitro model using PBECs, we first found that the cAMP level (Fig. 4) was significantly higher with pretreatment with IND or TH, compared with the control or CSE-stimulated group. Besides, exposure of PBECs to CSE increased inflammatory cytokine IL-8 production (Fig. 5), which was attenuated by IND (Fig. 5A) or TH (Fig.5B). Blocking the cAMP-AC-PKA pathway by adding KH7 (AC inhibi-

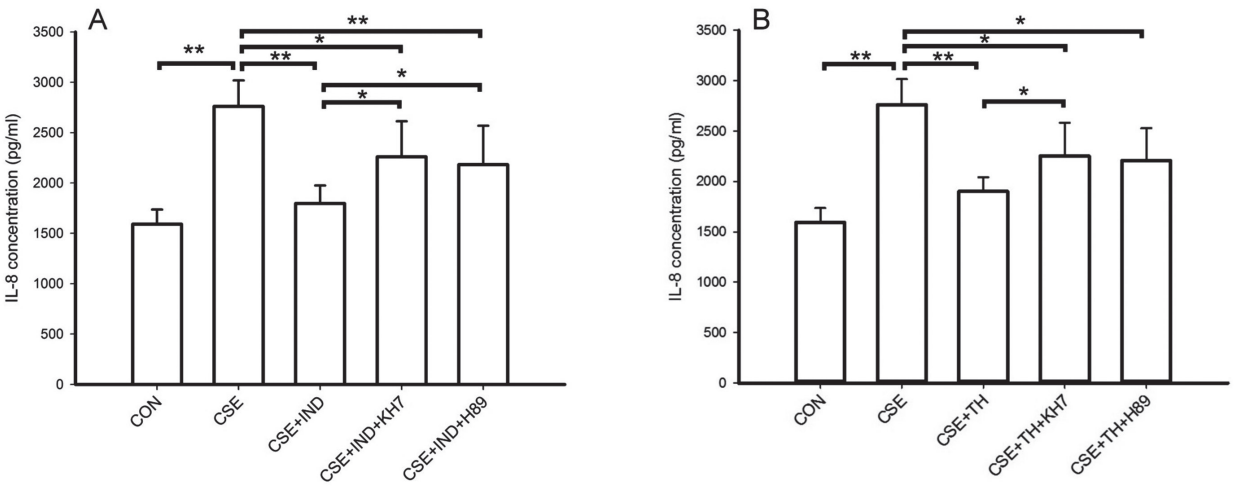

Fig. 5. Treatment with (A) indacaterol maleate (IND) or (B) theophylline (TH) suppressed cigarette smoke extract (CSE)-induced increases in interleukin (IL)-8 production in primary bronchial epithelial cells (PBECs). Cells were exposed to 3% CSE with pretreatment with a vehicle, IND (100 nM) or TH (100 nM). KH7 (adenylyl cyclase inhibitor, 25 μM) or H89 (protein kinase A inhibitor, 10 μM) was used to observe its ability in alleviating the anti-inflammatory effect of IND or TH. Control groups (CON) were cells without stimulation and pretreatment. IL-8 production levels in cell lysates were analyzed by ELISA assay. Data in each group are mean ± SEM from 5-8 independent experiments. *, $p < 0.05$; **, $p < 0.01$.

tor) or H89 (PKA inhibitor) alleviated this anti-inflammatory effect of IND (Fig. 5A) or TH (Fig, 5B).

Discussion

In the present study, we have clearly demonstrated that, in the mice model of 4-week CS exposure, treatment with IND, a LABA, or TH markedly alleviated airway inflammation, as evidenced by reductions in cell infiltration and peribronchial collagen deposition, and in inflammatory cells accumulation and protein leakage in BALF, although the synergistic effect of adding TH to IND did not reach statistical significance. Besides, in our cell model, CSE induced an increase of IL-8 production in PBECs, which was inhibited by IND or TH via a cAMP-AC-PKA pathway. Taken together, these in vivo and in vitro data suggest that IND and TH may exert a potent inhibitory effect on CS-induced airway inflammation through regulating the cAMP-AC-PAK pathway.

Compared with other LABAs, IND is a once-daily ultra-LABA that is most effective in improving lung function and symptom burden, and in reducing exacerbation in moderate to severe COPD [8-9, 24, 25], and was originally approved for clinical use as monotherapy for patients with COPD [26]. Decreasing the frequency of exacerbations is one of the main goals of treatment for COPD patients, and current clinical evidence supports the possibility that the effects of LABA on symptom severity, hyperinflation and mucociliary clearance may contribute to decreasing exacerbations [27]. In addition, while exacerbation of COPD is related to increased airway inflammation [7], the anti-inflammatory effects of LABA and its mechanism are also widely discussed. Our previous studies have shown that inhaled corticosteroid (ICS)/LABA could reduce IL-8 and matrix metalloprotease (MMP)-9 in induced sputum from COPD patients [28], restore the reduction of histone deacetylase (HDAC) activity, and inhibit H_2O_2-induced mediator release in alveolar

macrophages [29]. Besides, olodaterol, another ultra-LABA, also attenuated acute (4-day) CS exposure-induced pulmonary cell influx and pro-inflammatory mediator release in a guinea pig model [30]. By increasing levels of cAMP and PKA, stimulation of beta-2 adrenergic receptors also exerted largely inhibitory effects on cells of the immune system [31]. Our results support the existing evidence that LABA attenuated CS exposure-induced lung inflammation via the cAMP-AC-PKA pathway. Of note, our subchronic (4-week) CS-exposed murine model more adequately mimicked the process of COPD.

Nevertheless, the current COPD guideline recommends combination therapy rather than monotherapy for patients with high symptom burdens, who suffer from frequent exacerbations [11, 32-34]. For instance, roflumilast, a selective PDE4 inhibitor, is also recommended for those who have poor pulmonary function or chronic bronchitis that remains uncontrolled with triple (LAMA/LABA/ICS) inhaled therapy [11], given the evidence that roflumilast can reduce the rate of exacerbation of moderate or severe COPD and increase FEV1 by 48 mL compared with placebo. [12, 35]. More importantly, the principal action of this selective PDE4 inhibitor in reducing exacerbation is believed to be associated with reducing airway inflammation by inhibiting the breakdown of intracellular cAMP [36]. In our study, TH, a nonselective PDE inhibitor, which is more widely used worldwide probably because of its lower price, demonstrated its inhibitory effect on CS-induced airway inflammation via regulating the cAMP level. Furthermore, we have shown that the cAMP-AC-PKA pathway plays a key role in airway inflammation.

The cAMP-AC-PKA pathway is traditionally thought of as the main pathophysiology for airway smooth muscle cells relaxation and bronchodilatation [37]. Emerging evidence, including our study, shows that activation of the cAMP-AC-PKA pathway can contribute to a reduced level of inflammatory cytokines in vitro [10, 38, 39]. 8-Br-cAMP, an agonist analog to PKA, caused a small but significant decrease in swine barn dust-stimulated IL-8 in an alveolar epithelial cell line [38]. Another study also showed that 8-Br-cAMP decreased hog dust extract (HDE)-stimulated IL-6, IL-8, and tumor necrosis factor (TNF)-α released in airway epithelial cells. The author also demonstrated that 8-Br-cAMP blocked HDE-stimulated IL-6 and keratinocyte-derived chemokine release in precision-cut mouse lung slices [39]. These studies also supported our findings that activation of the cAMP-AC-PKA pathway via IND and TH can inhibit CS-induced airway inflammation *in vivo* and *in vitro*.

Although the synergistic effect of adding TH to IND did not reach statistical significance, there was still a trend toward decreased total cell counts, especially macrophages, in the BALF (Fig. 1 and 2). Macrophages play essential roles in phagocytosis, innate and adaptive immunity, and surfactant homeostasis. Prior classification schemes proposed the existence of 2 phenotypes, namely classically activated M1 macrophages that arise in response to interferon (IFN)-γ, IL-6, IL-1β and TNF-α to initiate phagocytosis; and alternatively, activated M2 macrophages that arise in response to stimulation with IL-4, IL-10, IL-13, and TGF-β1, which is associated with tissue repair [40-41]. De Cunto G and colleagues found that a large population of M1 macrophages predominates in the lung using an emphysema murine model after chronic CSE [42]. A recent study also

showed that increased cAMP alone can increase IL-4-dependent M2 marker expression through a PKA/C/EBPβ/CREB-dependent pathway in murine macrophages [43]. Taken together, combining IND and TH might inhibit CS-induced M1 macrophage accumulation via activating the cAMP-PKA pathway.

There are several limitations to our study. First, although the study has demonstrated the anti-inflammatory effect of IND and TH in vitro and in vivo, the clinical evidence is still lacking. Still, our study has provided further information about the possible mechanism of pharmacological intervention in reducing exacerbation. Another limitation is that the CS-exposed mice received daily treatment with IND and/or TH from day 1 in this study, which differs from a clinical scenario in which patients would have a long smoking history before using medication. While we recognize this difference, still, our results are in good agreement with the clinical benefits of IND or TH used in addition to bronchodilator action. Third, CS induces multiple cytokines and causes persistent inflammatory cells accumulation and tissue damage [5]. We did not measure cytokines other than IL-8, yet it remains a key cytokine induced by CS that is deeply involved in the COPD pathogenesis and has a strong association with COPD exacerbation [44]. Fourth, we did not investigate whether adding TH to IND in a cell study had a synergistic effect, since the murine model showed a trend only, without statistical significance.

Conclusion

In conclusion, both IND and TH inhibited CS-induced airway inflammation through regulating cAMP and the AC-PKA pathway.

Acknowledgements

This study was supported by a grant from the Ministry of Science and Technology, Taiwan (MOST 103-2314-B-075-054).

Conflicts of Interest

The authors declare that they have no conflicts of interest.

Author Contributions

Yu-Jung Lin, Kang-Cheng Su and Yi-Han Hsiao: conception and design, conducting experiments, data analysis and interpretation, writing of the manuscript. Yi-Han Hsiao had final responsibility for the decision to submit for publication.

References

1. López-Campos JL, Tan W, Soriano JB. Global burden of COPD. Respirology 2016; 21: 14-23.
2. Rennard SI, Togo S, Holz O. Cigarette smoke inhibits alveolar repair: a mechanism for the development of emphysema. Proc Am Thorac Soc 2006; 3: 703-708.
3. Hsiao YH, Tseng CM, Su KC, *et al*. Glycopyrronium bromide inhibits lung inflammation and small airway remodeling induced by subchronic cigarette smoke exposure in mice. Respir Physiol Neurobiol 2018; 249: 16-22.
4. Perng DW, Chang TM, Wang JY, *et al*. Inflammatory role of AMP-activated protein kinase signaling in an experimental model of toxic smoke inhalation injury. Crit Care Med 2013; 41: 120-132.
5. Barnes PJ. Immunology of asthma and chronic obstructive pulmonary disease. Nat Rev Immunol 2008; 8: 183-192.
6. Hogg JC, Chu F, Utokaparch S, *et al*. The nature of small-airway obstruction in chronic obstructive pulmonary

disease. N Eng J of Med 2004; 350: 2645-2653.
7. Fujimoto K, Yasuo M, Urushibata K, *et al*. Airway inflammation during stable and acutely exacerbated chronic obstructive pulmonary disease. Eur Respir J 2005; 25: 640-646.
8. Chapman KR. Rennard SI, Dogra A, *et al*. Long-term safety and efficacy of indacaterol, a long-acting beta2-agonist, in subjects with COPD: a randomized, placebo-controlled study. Chest 2011; 140: 68-75.
9. Donohue JF, Fogarty C, Lotvall J, *et al*. Once-daily bronchodilators for chronic obstructive pulmonary disease: indacaterol versus tiotropium. Am J Respir Crit Care Med 2010; 182: 155-162.
10. Oldenburger A, Roscioni SS, Jansen E, *et al*. Anti-inflammatory role of the cAMP effectors Epac and PKA: implications in chronic obstructive pulmonary disease. PloS one 2012; 7: e31574.
11. Global Initiative for Chronic Obstructive Lung Disease. 2021 Global Strategy for Prevention, Diagnosis and Management of COPD. 2021. https://goldcopd.org/2021-gold-reports/. Accessed January 15, 2021.
12. Janjua S, Fortescue R, Poole P. Phosphodiesterase-4 inhibitors for chronic obstructive pulmonary disease. Cochrane Database Syst Rev 2020 May 1; 5(5): CD002309.
13. Grootendorst DC, Gauw SA, Verhoosel RM, *et al*. Reduction in sputum neutrophil and eosinophil numbers by the PDE4 inhibitor roflumilast in patients with COPD. Thorax 2007; 62: 1081-1087.
14. Yano Y, Yoshida M, Hoshino S, *et al*. Anti-fibrotic effects of theophylline on lung fibroblasts. Biochem Biophys Res Commun 2006; 341: 684-690.
15. Moon HG, Kim YS, Choi JP, *et al*. Aspirin attenuates the anti-inflammatory effects of theophylline via inhibition of cAMP production in mice with non-eosinophilic asthma. Exp Mol Med 2010; 42: 47-60.
16. Al Shoyaib A, Archie SR, Karamyan VT. Intraperitoneal route of drug administration: should it be used in experimental animal studies? Pharm Res 2019; 37: 12.
17. Stessin AM, Zippin JH, Kamenetsky M, *et al*. Soluble adenylyl cyclase mediates nerve growth factor-induced activation of Rap1. J Biol Chem 2006; 281: 17253-8.
18. Tannheimer SL, Wright CD, Salmon M. Combination of roflumilast with a beta-2 adrenergic receptor agonist inhibits proinflammatory and profibrotic mediator release from human lung fibroblasts. Respir Res 2012; 13: 28.
19. Perng DW, Wu YC, Tsai MC, *et al*. Neutrophil elastase stimulates human airway epithelial cells to produce PGE2 through activation of p44/42 MAPK and upregulation of cyclooxygenase-2. Am J Physiol Lung Cell Mol Physiol 2003; 285: L925-30.
20. Yang SR, Chida AS, Bauter MR, *et al*. Cigarette smoke induces proinflammatory cytokine release by activation of NF-kappaB and posttranslational modifications of histone deacetylase in macrophages. Am J Physiol Lung Cell Mol Physiol 2006; 291: L46-57.
21. Kode A, Rajendrasozhan S, Caito S, *et al*. Resveratrol induces glutathione synthesis by activation of Nrf2 and protects against cigarette smoke-mediated oxidative stress in human lung epithelial cells. Am J Physiol Lung Cell Mol Physiol 2008; 294: L478-88.
22. Frankenfeld CN, Rosenbaugh MR, Fogarty BA, *et al*. Separation and detection of peroxynitrite and its metabolites by capillary electrophoresis with UV detection. J Chromatogr A. 2006; 1111: 147-52.
23. Yu YB, Liao YW, Su KH, *et al*. Prior exercise training alleviates the lung inflammation induced by subsequent exposure to environmental cigarette smoke. Acta Physiol (Oxf) 2012; 205: 532-540.
24. Han J, Dai L, Zhong N. Indacaterol on dyspnea in chronic obstructive pulmonary disease: a systematic review and meta-analysis of randomized placebo-controlled trials. BMC Pulm Med 2013 Apr 25; 13: 26.
25. Donohue JF, Betts KA, Du EX, *et al*. Comparative efficacy of long-acting β2-agonists as monotherapy for chronic obstructive pulmonary disease: a network meta-analysis. Int J Chron Obstruct Pulmon Dis 2017; 12: 367-381.
26. Burkes RM, Panos RJ. Ultra long-acting β-agonists in chronic obstructive pulmonary disease. J Exp Pharmacol 2020; 12: 589-602.
27. Beeh KM, Burgel PR, Franssen FME, *et al*. How do dual long-acting bronchodilators prevent exacerbations of chronic obstructive pulmonary disease? Am J Respir Crit Care Med 2017; 196: 139-149.
28. Perng DW, Tao CW, Su KC, *et al*. Anti-inflammatory effects of salmeterol/fluticasone, tiotropium/fluticasone or tiotropium in COPD. Eur Respir J 2009; 33: 778-84.
29. Perng DW, Su KC, Chou KT, *et al*. Long-acting β2 agonists and corticosteroids restore the reduction of

histone deacetylase activity and inhibit H_2O_2-induced mediator release from alveolar macrophages. Pulm Pharmacol Ther 2012; 25: 312-8.

30. Wex E, Kollak I, Duechs MJ, *et al*. The long-acting β2-adrenoceptor agonist olodaterol attenuates pulmonary inflammation. Br J Pharmacol 2015; 172: 3537-47.
31. Lorton D, Bellinger DL. Molecular mechanisms underlying β-adrenergic receptor-mediated cross-talk between sympathetic neurons and immune cells. Int J Mol Sci 2015; 16: 5635-65.
32. Nici L, Mammen MJ, Charbek E, *et al*. Pharmacologic management of chronic obstructive pulmonary disease. An official American Thoracic Society clinical practice guideline. Am J Respir Crit Care Med 2020; 201: e56-e69.
33. Lipson DA, Barnhart F, Brealey N, *et al*. Once-daily single-inhaler triple versus dual therapy in patients with COPD. N Engl J Med 2018; 378: 1671-1680.
34. Rabe KF, Martinez FJ, Ferguson GT, *et al*. Triple inhaled therapy at two glucocorticoid doses in moderate-to-very-severe COPD. N Engl J Med 2020; 383: 35-48.
35. Calverley PM, Rabe KF, Goehring UM, *et al*. Roflumilast in symptomatic chronic obstructive pulmonary disease: two randomised clinical trials. Lancet 2009; 374: 685-94.
36. Rabe KF. Update on roflumilast, a phosphodiesterase 4 inhibitor for the treatment of chronic obstructive pulmonary disease. Br J Pharmacol 2011; 163: 53-67.
37. Billington CK, Ojob OO, Penn RB, *et al*. cAMP Regulation of airway smooth muscle function. Pulm Pharmacol Ther 2013; 26: 112-120.
38. Burvall K, Palmberg L, Larsson K. Effects by 8-bromo-cyclicAMP on basal and organic dust-induced release of interleukin-6 and interleukin-8 in A549 human airway epithelial cells. Respir Med 2003 Jan; 97: 46-50.
39. Wyatt TA, Poole JA, Nordgren TM, *et al*. cAMP-dependent protein kinase activation decreases cytokine release in bronchial epithelial cells. Am J Physiol Lung Cell Mol Physiol 2014; 307: L643-51.
40. Pechkovsky DV, Prasse A, Kollert F, *et al*. Alternatively activated alveolar macrophages in pulmonary fibrosis-mediator production and intracellular signal transduction. Clin Immunol 2010; 137: 89-101.
41. Wynn TA, Vannella KM. Macrophages in tissue repair, regeneration, and fibrosis. Immunity 2016; 44: 450-62.
42. De Cunto G, Cavarra E, Bartalesi B, *et al*. Alveolar macrophage phenotype and compartmentalization drive different pulmonary changes in mouse strains exposed to cigarette smoke. COPD 2020; 17: 429-443.
43. Polumuri S, Perkins DJ, Vogel SN. cAMP levels regulate macrophage alternative activation marker expression. Innate Immun 2021 Feb; 27(2): 133-142. doi: 10.1177/1753425920975082. Epub 2020 Nov 26.
44. Perng DW, Chen PK. The relationship between airway inflammation and exacerbation in chronic obstructive pulmonary disease. Tuberc Respir Dis (Seoul) 2017; 80: 325-335.

Clinical Application of High-Flow Nasal Cannula Oxygen Therapy for Patients with Blunt Chest Injury: A Prospective Study

Yin-Chi Lee[1,2,*], Chun-Fu Chang[2,4,5,*], Chien-Ho Tsai[3], Shih-Chieh Chang[2,4,5]
Hsin-Yi Chang[2,6], Yi-Chun Lai[2,4,5]

Introduction: Blunt chest injury (BCI) is associated with a high risk of mortality. High-flow nasal cannula (HFNC) oxygen therapy can be used to reduce the risk of respiratory failure due to hypoxemia, and can significantly reduce the need for intubation compared with general oxygen therapy and the use of a non-invasive positive pressure breathing apparatus. However, it is not widely known whether HFNC can be used in trauma-related hypoxemia.

Methods: We performed a cross-sectional study of patients with BCI but without hypercapnia, and compared HFNC therapy with standard oxygen therapy (control group). The primary outcome was the ratio of the proportion of patients intubated in each group; secondary outcomes included mortality in the intensive care unit (ICU), duration of hospital and ICU stay, and other complications.

Results: A total of 74 patients fulfilled the BCI criteria and were divided into the HFNC and control groups, with 24 and 50 patients, respectively. Findings revealed a lower respiratory failure rate requiring intubation in the HFNC group (4.2% vs. 10%, p=0.657). A trend toward a shorter length of ICU and hospital stay in the HFNC group was noted, as well as lower incidence of pneumonia (25% vs. 40%, p=0.206). Hemodynamic changes in the control group revealed an increased heart rate and respiratory rate 48 hours later, and an increased respiratory rate after 72 hours.

Conclusion: This is the first study in Taiwan to investigate initial HFNC use in patients with BCI. Usage of HFNC for 48 hours exhibited beneficial hemodynamic changes with a lower respiratory and heart rate, and a trend toward a lower rate of intubation, less pneumonia risk, a shorter hospital and ICU stay, and a lower 30-day mortality rate. ***(Thorac Med 2022; 37: 13-20)***

Key words: Blunt chest injury, chest trauma, high-flow nasal cannula, respiratory failure, ventilation

[1]Graduate Institute of Clinical Medical Sciences, College of Medicine, Chang Gung University, Taoyuan, Taiwan, [2]Department of Critical Care Medicine, National Yang-Ming Chiao Tung University Hospital, Yi-Lan, Taiwan, [3]Division of Chest Surgery, Department of Surgery, National Yang-Ming Chiao Tung University Hospital, Yi-Lan, Taiwan, [4]Division of Chest Medicine, Department of Internal Medicine, National Yang-Ming Chiao Tung University Hospital, Yi-Lan, Taiwan, [5]Faculty of Medicine, School of Medicine, National Yang-Ming Chiao Tung University, Taipei, Taiwan, ROC, [6]Graduate Bachelor of Sciences, School of Respiratory Therapy. Taipei Medical University, Taipei, Taiwan.

Address reprint requests to: Dr. Yi-Chun Lai, Division of Chest Medicine, Department of Internal Medicine, National Yang-Ming Chiao Tung University Hospital, Yi-Lan, Taiwan, No. 169, Siaoshe Rd., Yi-lan City, Yi-lan Country 26058, Taiwan (R. O. C.)

*These authors contributed equally to this work.

Introduction

Blunt chest injury (BCI) has varied mortality rates (4-36%) and morbidity, as reported in different studies [1-3]. BCI involves bony and non-bony structure injuries, including those from direct impact, thoracic compression, rapid deceleration, and blast injury [4]. There are several types of mechanisms that result in rib fracture, flail chest, pneumothorax, hemothorax, lung contusion, soft tissue contusion, and sternal fracture in BCI [5-7]. The American Association for the Surgery of Trauma (AAST) has created a grading system to identify the severity of chest wall injuries. Patients with BCI are complicated with respiratory issues, such as pain and immobilization, leading to pneumonia, poor ventilation, decreased respiratory volume, and atelectasis [8]. Thus, BCI often results in an increase in hospital stay, intensive care unit (ICU) stay, use of mechanical ventilation (MV), and mortality [9-12]. Some studies have reported that every additional rib fracture in the elderly increased the incidence of pneumonia and mortality by 27% and 19%, respectively [13-14]. Treatment for BCI includes adequate pain control, surgical intervention, chest care, respiratory care, and early mobilization [15-16].

Non-invasive ventilation (NIV) can improve ventilation and gas exchange, and had fewer complications, such as pneumonia or barotrauma, compared with MV in a mixed ICU (12% trauma patients) [17-18]. A randomized controlled study revealed that NIV with a helmet increased oxygenation, improved tolerance, and decreased complications compared to use of a face mask in patients with chest trauma [19]. High-flow nasal cannula (HFNC) can offer humidified oxygen, a higher flow rate of approximately 30-100 L/min, a higher fraction of inspired oxygen (FiO_2), and positive end expiratory pressure to prevent alveoli collapse [20-22]. HFNC has demonstrated better tolerance in increasing comfort and nasal prong use than NIV.

There are limited studies [23-24] discussing HFNC in patients with BCI. Therefore, we designed a prospective study to evaluate the clinical application of HFNC in patients with BCI, and its association with intubation rate and ICU stay.

Materials and Methods

Study design

This prospective study was conducted in a regional hospital with a surgical ICU with 18 beds. We included BCI patients with (1) a standard definition of BCI, including chest wall injury: chest contusion, hemothorax, rib fracture, flail chest, hematoma, sternal fracture, clavicle fracture; airway injury: bronchus tear, heart injury, cardiac tamponade, heart contusion, pericardial effusion; vascular injury: traumatic aortic tear, thoracic aortic injury, aortic dissection; esophageal injury; and diaphragm injury; (2) written informed consent; (3) an age of more than 20 years; (4) partial pressure of carbon dioxide ($PaCO_2$) ≤50 mmHg, and (5) a Glasgow Coma Scale (GCS) ≥12. Exclusion criteria were (1) aged younger than 20 years, (2) unstable hemodynamics, (3) $PaCO_2$ >50 mmHg, (4) GCS <12, (5) intubation due to acute respiratory failure, (6) pulmonary edema, and (7) any contraindication for HFNC.

Once the patient was admitted to the surgical ICU, we followed the laboratory data, including Acute Physiology and Chronic Health Evaluation II (APACHE II), Injury Severity Score (ISS), Thoracic Trauma Severity Score (TTSS), body temperature, blood pressure, respiratory rate, arterial blood gas (initial, 24

hours after admission, 72 hours after admission), coma scale, PaO_2/FiO_2 (arterial oxygen partial pressure/fraction of inspired oxygen) ratio (P/F ratio), chest radiography, chest computerized tomography, and basic biochemistry data.

The criteria for the decision to intubate in the HFNC group included: (1) unstable hemodynamics, (2) worsening coma scale, (3) respiratory distress, such as rapid respiratory rate ≥40/minute (min), increased secretions, increased work of breathing, accessory muscle use, and abnormal arterial blood gas data, (4) the in-charge doctor's decision to intubate. The initial HFNC setting was a flow of 50 liters (L)/min, FiO_2 of 50%, and pulse oximetry (SpO_2) higher than 95%.

The control group was gathered from August 2018 to June 2019, and was given standard care, except for HFNC. The HFNC group was collected from July 2019 to August 2021.

The primary endpoint was the intubation rate between HFNC and the other oxygen support systems. We also analyzed the outcomes of ICU stay, pneumonia risk, mortality, and changes in hemodynamic and vital signs at 48 h and 72 h after admission.

Statistical analysis

SPSS (version 22; IBM Corporation, Armonk, NY, USA) was used for statistical analysis of the clinical data. Data were calculated as frequencies for categorical variables, and median (standard deviation) for continuous variables. Categorical variables were compared using the chi-square test or Fisher's exact test, and continuous variables were compared using an independent unpaired t-test.

Results

Data on trauma patients admitted to the surgical ICU in our hospital was collected between August 2018 and August 2021 (Figure 1). There was a total of 746 patients, 528 of which were excluded due to lack of BCI. Of the remaining 218 patients, 88 were excluded due to missing data, and 56 because they had an endotracheal tube inserted in the ER. Finally, a total of 74 patients fulfilled the BCI criteria; we divided these into the control group and HFNC group, with 50 and 24 patients, respectively.

During the enrolled period for the control group (August 2018-June 2019), a total of 708

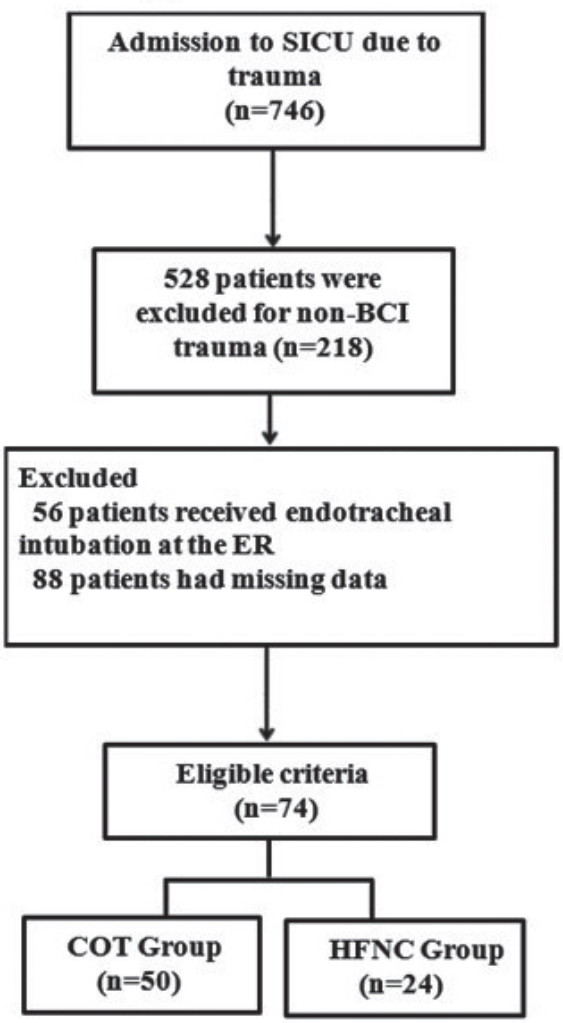

Fig. 1. Blunt chest injury flow chart.

patients were admitted to ICU for traumatic injury. We excluded 526 of these patients due to a lack of BSI, 54 who had had an endotracheal tube in the ER and 78 with missing data. There were a total of 50 cases remaining in the control group. During the HFNC group study period (July 2019 to August 2021), there were 38 patients with HFNC use. We excluded 2 patients without BSI, 2 with endotracheal tube insertion in the ER, and 10 patients with missing data. There was a total of 24 patients in the HFNC group.

The demographic characteristics are presented in Table 1. Gender, age, APACHE II,

Table 1. Demographics of the Patients with Blunt Chest Injury Under high-flow Nasal Cannula or Standard Oxygen Therapy

	HFNC (n=24)	Control (n=50)	*P* value
Characteristic			
Male sex, °n° (%)	15 (62.5%)	32 (64%)	0.9
Age (years old)	63.6±17.6	59.7±23.3	0.425
Height (cm)	163.8±7.3	162.8±8.7	0.635
Body Weight (kg)	62.2±12.4	67.7±16.4	0.116
Body mass index (kg/m^2)	24.2±7.4	33±14.3	0.01
APACHE II	7.7±4.1	7.5±4.4	0.861
ISS	16.6±7.5	21.7±7	0.06
TTSS	9±2.6	9.4±2.9	0.62
Mechanism of injury, °n° (%)			
Traffic accident	16 (66.7%)	42 (84%)	0.09
Fall	8 (33.3%)	8 (16%)	0.09
Arterial blood gas			
pH	7.38±0.04	7.36±0.04	0.058
PaO_2 (mmHg)	103.7±29.1	111.4±53.6	0.517
$PaCO_2$ (mmHg)	39.1±4.9	43.3±7.6	0.017
PaO_2/FiO_2 (mmHg)	338.1±91	318.1±124.9	0.486
Chest Injury, °n° (%)			
Lung contusion	8 (33.3%)	28 (56%)	0.068
Rib fracture			
1-3 ribs	5 (20%)	3 (12%)	0.702
3-6 ribs	7 (29%)	10 (45%)	0.253
>6 ribs	12 (50%)	9 (40%)	0.536
Flail chest	3 (12.5%)	7 (14%)	1
Pneumothorax	9 (37.5%)	31 (62%)	0.048
Hemothorax	12 (50%)	31 (62%)	0.327
Hemopneumothorax	5 (20.8%)	21 (42%)	0.074
Comorbidities			
Pulmonary Disease, n° (%)	2 (8.3%)	5 (10%)	1
Cancer, n° (%)	3 (12.5%)	4 (8%)	0.675
Stroke, n° (%)	0 (0%)	4 (8%)	0.297
Hypertension, n° (%)	11 (45%)	21 (42%)	0.755
Cardiovascular, n° (%)	2 (8.3%)	11 (22%)	0.2
Diabetes mellitus, n° (%)	7 (29%)	9 (18%)	0.275

Acronyms: n, number; HFNC, high-flow nasal cannula; cm, centimeter; kg, kilogram; APACHE II, Acute Physiology and Chronic Health Evaluation II; ISS, Injury Severity Score; TTSS, Thoracic Trauma Severity Score; mean ± SD, mean ± standard deviation; FiO_2, fraction of inspired oxygen; PaO_2, arterial oxygen partial pressure; SpO_2, pulse oximetry; $PaCO_2$, partial pressure of carbon dioxide; IQR, interquartile range.

ISS, and TTSS were not significantly different between the control and HFNC groups. However, a lower body mass index (BMI) was found in the HFNC group (24.2±7.4 kg/m^2 vs. 33±14.3 kg/m^2, p=0.01). The mechanism of injury was mostly related to traffic accidents (84% in the control group and 66.7% in the HFNC group, p=0.09). A lower partial pressure of carbon dioxide ($PaCO_2$) was noted in the HFNC group (39.1±4.9 mmHg vs. 43.3±7.6 mmHg, p=0.017). The most common chest injuries in the control group were pneumothorax (62%), hemothorax (62%), and lung contusion (56%), and in the HFNC group, hemothorax (50%), >6 rib fractures (50%), and pneumothorax (37.5%). More pneumothorax patients were found in the control group than in the HFNC group (62% vs. 37.5%, p=0.048). Comorbidities did not differ between the 2 groups.

There was only 1 case of death within 30 days in the control group and none in the HFNC group (Table 2). The patient was an 89-year-old man with hypertension, type 2 diabetes mellitus, and chronic obstructive pulmonary disease. He had a right second to eleventh rib fracture with hemothorax status-pigtail drainage first (APACHE II: 18, ISS: 16, TTSS: 9). We were unable to resuscitate him after 7 days of admission, and he died of pneumonia with multiple organ failure. The intubation rate for respiratory failure and NIPPV use, ICU stay, and hospital days tended to increase in the control group; however, the difference was not significant. In the HFNC group, there was a trend toward a lower respiratory failure rate requiring intubation (4.2% vs. 10%, p=0.657), a shorter hospital and ICU length of stay, and a lower occurrence of pneumonia (25% vs. 40%, p=0.206).

Arterial blood gas after 48 h (Table 3) and 72 h (Table 4) showed no significant change between the control and HFNC groups, in terms of pH, PaO_2, SpO_2, FiO_2, and PaO_2/FiO_2. Hemodynamic changes showed an increase in heart rate and respiratory rate in the control group at 48 h (Table 5) and an increased respiratory rate in the control group at 72 h (Table 6).

Discussion

This is the first study to report the clinical application of HFNC in patients with BCIs in Taiwan. The outcomes of patients with BCI in

Table 2. Outcome of Blunt Chest Injury Patients

	HFNC (n=24)	Control (n=50)	*P* value
Reason for intubation, °n° (%)			
Operation	2 (8.3%)	9 (18%)	0.486
Respiratory failure	1 (4.2%)	5 (10%)	0.657
NIPPV use, n (%)	0 (0%)	2 (4%)	1
MV use >20 day, n (%)	0 (0%)	2 (4%)	1
ICU LOS (days)	5.8±6.2	6.7±6	0.578
Hospital LOS (days)	13±8.8	16±9.9	0.359
Pneumonia, n (%)	6 (25%)	20 (40%)	0.206
30 days mortality, n (%)	0 (0%)	1 (2%)	1

Acronyms: HFNC, high-flow nasal cannula; n, number; NIPPV, non-invasive positive pressure ventilator; MV, mechanical ventilator; ICU, intensive care unit; LOS, length of stay.

Table 3. The Arterial Blood gas Data After HFNC and Standard Treatment After 48 Hours Later

	HFNC (n°=23)	Control (n°=36)	*P* value
pH	7.39±0.04	7.37±0.05	0.111
PaO_2 (mmHg)	107.5±26.8	100.8±36.5	0.456
SpO_2 (%)	97±1.8	96±3.2	0.051
FiO_2 (%)	35.6±7	37.7±8.5	0.345
PaO_2/FiO_2 (mmHg)	306±82	282.6±96	0.321

Acronyms: HFNC, high-flow nasal cannula; n, number; FiO_2, fraction of inspired oxygen; °PaO_2, arterial oxygen partial pressure; SpO_2, pulse oximetry.

Table 4. Arterial Blood gas Data After HFNC and Standard Treatment 72 Hours Later

	HFNC (n°=22)	Control (n°=34)	*P* value
pH	7.40±0.02	7.37±0.78	0.145
PaO_2 (mmHg)	100.0±24.0	102.0±30.0	0.837
SpO_2 (%)	97±1.8	96±2.2	0.456
FiO_2 (%)	36.1±8.4	36.6±9.4	0.855
PaO_2/FiO_2 (mmHg)	291.0±93.5	298.3±102.4	0.801

Acronyms: HFNC, high-flow nasal cannula; n, number; FiO_2, fraction of inspired oxygen; PaO_2, arterial oxygen partial pressure; SpO_2, pulse oximetry.

Table 5. The Vital Signs After HFNC and Standard Treatment 48 Hours Later

	HFNC (n°=20)	Control (n°=50)	*P* value
Heart rate (beat/min)	79±13	88±2	0.038*
Respiratory rate (breaths/min)	17±4	21±5	0.001**
Arterial pressure (mmHg)			
Systolic	133±27	132±19	0.869
Diastolic	69±10	70±10	0.742

Acronyms: HFNC, high-flow nasal cannula; n, number.

Table 6. Vital Signs After HFNC and Standard Treatment 72 Hours Later

	HFNC (n°=24)	Control (n°=50)	*P* value
Heart rate (beat/min)	83±16	86±15	0.472
Respiratory rate (breaths/min)	16±3	20±4	0.002**
Arterial pressure (mmHg)			
Systolic	132±20	133±16	0.768
Diastolic	73±10	69±10	0.069

Acronyms: HFNC, high-flow nasal cannula; n, number.

the HFNC group showed no significant difference from those in the control group; however, there was a trend toward a lower intubation rate and pneumonia risk, a shorter hospital and ICU stay, and lower 30-day mortality in the HFNC group. After HFNC use, hemodynamic stability improved with a lower respiratory rate after 48 h and 72 h, and a lower heart rate after 48 h, compared to the control group. These findings suggest that HFNC is an optimal respiratory support for patients with BCI.

The indication for HFNC is acute hypoxemic respiratory failure (mainly pneumonia) [25-26], and post-extubation with a low risk of reintubation [27] . There have been few studies on the use of HFNC in BCI. MV has been used with 50% of trauma-related chest injury patients [28]. NIV is also a common oxygen support strategy in BCI to decrease morbidity and mortality [29]; it can decrease the rate of intubation and respiratory failure [30], and shorten ICU length of stay [31]. A review article found that NIV may be suitable for patients with BCI, but only those without neurologic defects, with stable hemodynamics, and with no respiratory distress [32]. HFNC is considered more comfortable for patients using only nasal prongs, compared to mask use. Nasal prongs are better tolerated by patients and help in quickly stabilizing their respiratory pattern and heart rate [24].

There are several limitations to our study. First, this was a single-hospital study with a small number of cases. Second, the study design was not blinded to the patient group or treatment teams.

Conclusion

This is the first study in Taiwan to discuss initial HFNC use in patients with BCI. After 48 hours of HFNC use, there was a favorable hemodynamic change with a lower respiratory and heart rate. Our findings showed a beneficial trend with a lessened need for intubation, a lower risk of pneumonia, a shorter ICU and hospital stay, and lower 30-day mortality.

Author Contributions

All authors made a significant contribution to the work reported, including conception, study design, execution, acquisition of data, analysis, and interpretation. All authors took part in drafting, revising, and critically reviewing the article; gave final approval of the version to be published; have agreed on the journal to which the article has been submitted; and agree to be accountable for all aspects of the work.

References

1. Ziegler DW, Agarwal NN. The morbidity and mortality of rib fractures. J Trauma 1994; 37(6): 975-979.
2. Adegboye VO, Ladipo JK, Brimmo IA, *et al*. Blunt chest trauma. Afr J Med Med Sci 2002; 31(4): 315-320.
3. Quaday KA. Morbidity and mortality of rib fracture. J Trauma 1995; 39(3): 617.
4. Oikonomou A, Prassopoulos P. CT imaging of blunt chest trauma. Insights Imaging 2011; 2(3): 281-295.
5. Ursic C, Curtis K. Thoracic and neck trauma. Part one. Int Emerg Nurs 2010; 18(1): 47-53.
6. Ursic C, Curtis K. Thoracic and neck trauma. Part two. Int Emerg Nurs 2010; 18(2): 99-108.
7. Battle CE, Hutchings H, Evans PA. Risk factors that predict mortality in patients with blunt chest wall trauma: a systematic review and meta-analysis. Injury 2012; 43(1): 8-17.
8. Easter A. Management of patients with multiple rib fractures. Am J Crit Care 2001; 10(5): 320-327; quiz 328-329.
9. Bulger EM, Arneson MA, Mock CN, *et al*. Rib fractures in the elderly. J Trauma 2000; 48(6): 1040-1046;

discussion 1046-1047.
10. Harrington DT, Phillips B, Machan J, *et al*. Factors associated with survival following blunt chest trauma in older patients: results from a large regional trauma cooperative. Arch Surg 2010; 145(5): 432-437.
11. Bayouth L, Safcsak K, Cheatham ML, *et al*. Early intravenous ibuprofen decreases narcotic requirement and length of stay after traumatic rib fracture. Am Surg 2013; 79(11): 1207-1212.
12. Geerts WH, Code KI, Jay RM, *et al*. A prospective study of venous thromboembolism after major trauma. New Engl J Med 1994; 331(24):1601-1606.
13. Yeh DD, Kutcher ME, Knudson MM, *et al*. Epidural analgesia for blunt thoracic injury--which patients benefit most? Injury 2012; 43(10): 1667-1671.
14. Wardhan R. Assessment and management of rib fracture pain in geriatric population: an ode to old age. Curr Opin Anaesthesiol 2013; 26(5): 626-631.
15. Gage A, Rivara F, Wang J, *et al*. The effect of epidural placement in patients after blunt thoracic trauma. J Trauma Acute Care Surg 2014; 76(1): 39-45; discussion 45-36.
16. Mohta M, Verma P, Saxena AK, *et al*. Prospective, randomized comparison of continuous thoracic epidural and thoracic paravertebral infusion in patients with unilateral multiple fractured ribs--a pilot study. J Trauma 2009; 66(4): 1096-1101.
17. Antonelli M, Conti G, Rocco M, *et al*. A comparison of noninvasive positive-pressure ventilation and conventional mechanical ventilation in patients with acute respiratory failure. New Engl J Med 1998; 339(7): 429-435.
18. Christensson P, Gisselsson L, Lecerof H, *et al*. Early and late results of controlled ventilation in flail chest. Chest 1979; 75(4): 456-460.
19. Liu Q, Shan M, Zhu H, *et al*. Noninvasive ventilation with a helmet in patients with acute respiratory failure caused by chest trauma: a randomized controlled trial. Sci Rep 2020; 10(1): 21489.
20. Helviz Y, Einav S. A systematic review of the high-flow nasal cannula for adult patients. Critical Care 2018; 22(1): 71.
21. Nishimura M. High-flow nasal cannula oxygen therapy in adults. J Intensive Care 2015; 3(1): 15.
22. Nishimura M. High-flow nasal cannula oxygen therapy in adults: physiological benefits, indication, clinical benefits, and adverse effects. Respir Care 2016; 61(4): 29-541.
23. Halub ME, Spilman SK, Gaunt KA, *et al*. High-flow nasal cannula therapy for patients with blunt thoracic injury: a retrospective study. Can J Respir Ther 2016; 52(4):110-113.
24. Hsu JM, Clark PT, Connell LE, *et al*. Efficacy of high-flow nasal prong therapy in trauma patients with rib fractures and high-risk features for respiratory deterioration: a randomized controlled trial. Trauma Surg Acute Care Open 2020; 5(1): e000460.
25. Frat JP, Thille AW, Mercat A, *et al*. High-flow oxygen through nasal cannula in acute hypoxemic respiratory failure. New Engl J Med 2015; 372(23): 2185-2196.
26. Ni YN, Luo J, Yu H, *et al*. Can high-flow nasal cannula reduce the rate of endotracheal intubation in adult patients with acute respiratory failure compared with conventional oxygen therapy and noninvasive positive pressure ventilation? A systematic review and meta-analysis. Chest 2017; 151(4): 764-775.
27. Hernández G, Vaquero C, González P, *et al*. Effect of postextubation high-flow nasal cannula vs conventional oxygen therapy on reintubation in low-risk patients: a randomized clinical trial. JAMA 2016; 315(13): 1354-1361.
28. Rico FR, Cheng JD, Gestring ML, *et al*. Mechanical ventilation strategies in massive chest trauma. Crit Care Clin 2007; 23(2): 299-315, xi, xi.
29. Nelson LD. Ventilatory support of the trauma patient with pulmonary contusion. Respir Care Clin N Am 1996; 2(3): 425-447.
30. Hernandez G, Fernandez R, Lopez-Reina P, *et al*. Noninvasive ventilation reduces intubation in chest trauma-related hypoxemia: a randomized clinical trial. Chest 2010; 137(1): 74-80.
31. Girard TD, Kress JP, Fuchs BD, *et al*. Efficacy and safety of a paired sedation and ventilator weaning protocol for mechanically ventilated patients in intensive care (Awakening and Breathing Controlled trial): a randomised controlled trial. Lancet 2008; 371(9607): 126-134.
32. Duggal A, Perez P, Golan E, *et al*. Safety and efficacy of noninvasive ventilation in patients with blunt chest trauma: a systematic review. Crit Care 2013; 17(4): R142.

Initiation of Systemic Corticosteroid Treatment in a Patient with Avian Influenza A (H7N9) Pneumonia, Guided by Blood CD4 Lymphocyte Count and Viral Load

Wei-Hsin Hung[1], Diahn-Warng Perng[2,3], Hsin-Kuo Ko[2,3]

Avian influenza A (H7N9) is a novel influenza A virus that has caused severe human illnesses in China since 2013. Neuraminidase inhibitor (NI) treatment, systemic steroid use, and intensive respiratory care have been used to manage severe avian influenza infection. The timing for initiation of steroid treatment remains uncertain, and the harmful effects of immune suppression and the potential for prolonging viral replication have been reported in the literature. Here, we reported a case of H7N9 influenza infection in a patient with acute respiratory distress syndrome who was supported with extracorporeal membrane oxygenation and given NIs and systemic steroid in accordance with the viral load and the blood CD4 lymphocyte count. ***(Thorac Med 2022; 37: 21-26)***

Key words: influenza, influenza A, H7N9, CD4 lymphocyte count, corticosteroid

Introduction

Avian influenza A (H7N9) is a novel influenza A virus that has caused severe illnesses in people in China since 2013. Systemic steroids are proposed as a valid therapeutic option due to their potential role in controlling the host inflammatory response, inhibiting pro-inflammatory cytokine production and restoring the inappropriately low endogenous cortisol levels, and compensating for critical illness-related corticosteroid insufficiency [1]. In the cellular response to influenza virus infection, CD4+ T lymphocytes provide help to B cells for production of antibodies to hemagglutinin and neuraminidase [2], and also promote the generation of virus-specific CD8+ cytotoxic T lymphocytes [3]. Clinically, influenza virus infection of peripheral blood mononuclear cells can lead to leukopenia and defects in cellular function. The administration of systemic steroid potentially suppresses the cellular immune response to influenza virus, and delays viral clearance. To our knowledge, the effect and the timing of systemic steroid use in influenza pneumonia are still controversial.

[1]Division of Chest Medicine, Department of Internal Medicine, Kaohsiung Veteran General Hospital, [2]Department of Chest Medicine, Taipei Veterans General Hospital, Taipei, Taiwan, ROC, [3]School of Medicine, National Yang-Ming University, Taipei, Taiwan, ROC
Address reprint requests to: Dr. Hsin-Kuo Ko, Chest department, Taipei Veteran General Hospital, No. 201, Sec. 2, Shipai Rd., Beitou Dist., Taipei City 112201, Taiwan (R.O.C.)

Here, we report a case of H7N9 infection in a patient with acute respiratory distress syndrome (ARDS) who was supported with extracorporeal membrane oxygenation (ECMO) and given neuraminidase inhibitors (NIs) for antiviral treatment. The systemic steroid treatment was used in accordance with the peripheral blood CD4 lymphocyte count and influenza viral load.

Case Report

A 45-year-old woman had a high fever and myalgia for 7 days before she traveled from Nanjing, China, to Taiwan on April 17, 2014. Influenza was suspected and the NI oseltamivir 75 mg twice per day was administered. However, pneumonia with ARDS developed quickly. Intubation with mechanical ventilator support was begun on April 21, 2014, and peramivir 600 mg per day was prescribed beginning April 22, 2014. The broad-spectrum antibiotics levofloxacin and imipenem were also prescribed. H7N9 infection was confirmed using quantitative real-time polymerase chain reaction (qPCR), and an exposure history in a poultry market was mentioned by the patient's husband. Chest X-ray revealed diffuse white-out at the left lung and an increased alveolar process at the right middle lobe (Figure 1A).

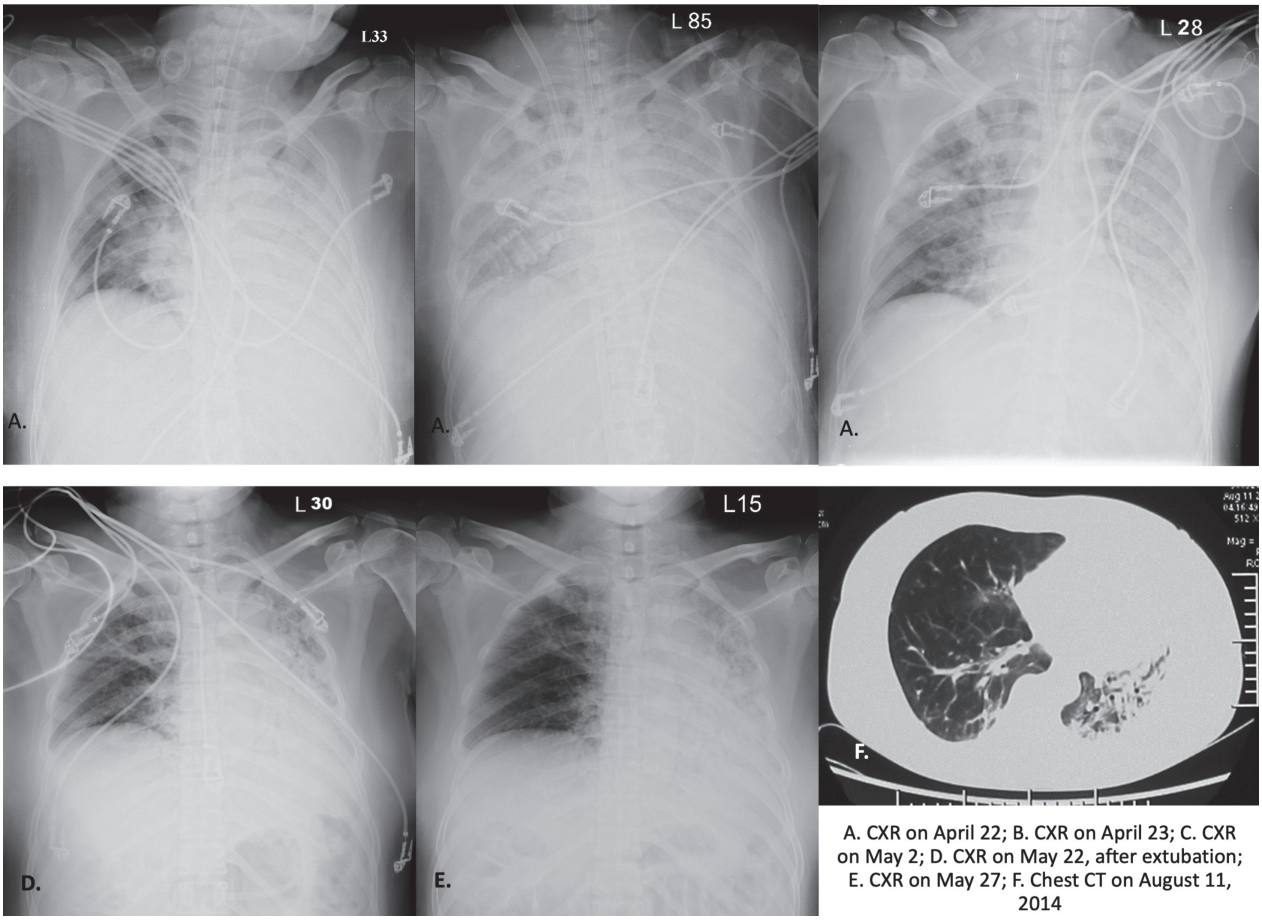

Fig. 1. A. Chest X-ray (CXR) on April 22, the day after intubation; B. CXR on April 23, the day ECMO began; C. CXR on May 2, the day ECMO was removed; D. CXR on May 22, after removal of the endotracheal tube; E. CXR on May 27, the day before discharge; F. Chest CT on August 11, 2014.

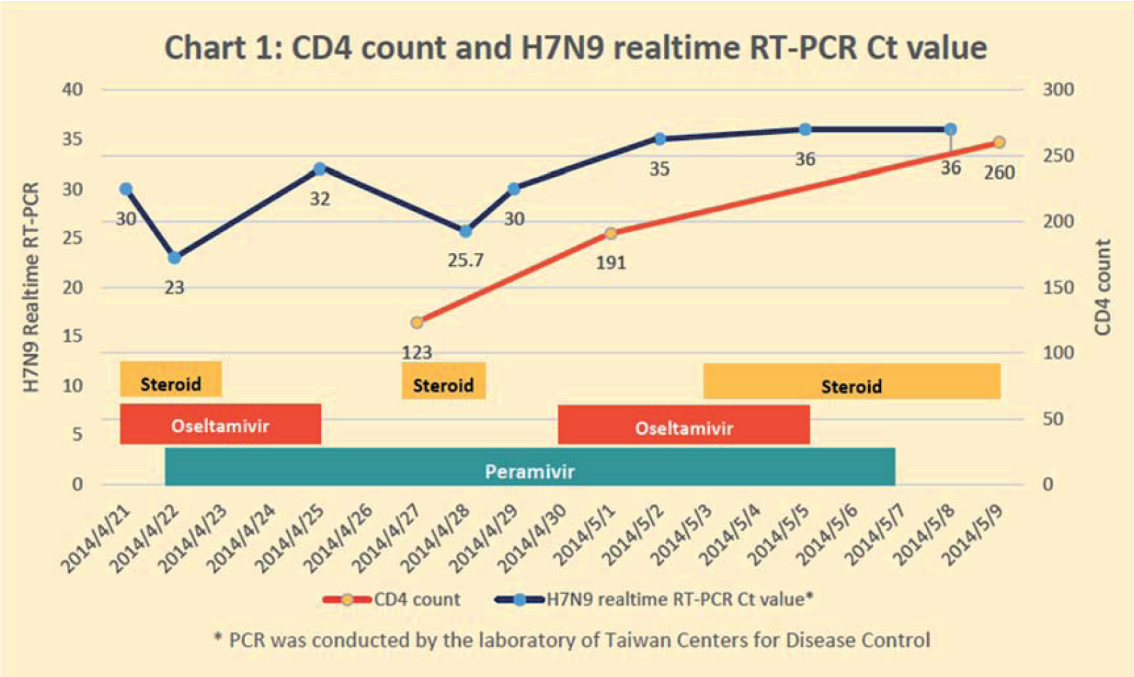

Chart. 1. CD4 count and H7N9 real-time RT-PCR Ct value (M gene)
Ct value of the H7N9 real-time PCR was negative if over 35.
Oseltamivir 75 mg twice per day from April 20 to April 25, and April 30 to May 5, 2014
Peramivir 600 mg once per day from April 22 to May 7, 2014
Methylprednisolone 1 mg/kg from April 21 to April 23, 2014, 2 mg/kg from May 3 to May 6, 2014, 0.5 mg/kg from May 6 to May 9, 2014

Ventilator management with a lung recruitment maneuver (RM) for severe hypoxemia (PaO_2/FiO_2 = 58 mm Hg) was initiated on April 22, 2014. ECMO was started because of rapid progression of pneumonia with persistent hypoxemia after RM. Chest X-ray revealed an alveolar process progression, even under dual NIs use as initial treatment and with the use of ECMO (Figure 1B). We frequently obtained a nasopharyngeal swab for H7N9 qPCR to monitor the patient's viral load (Chart 1). The Ct value of the M gene qPCR was collected and revealed a fluctuation initially. A systemic steroid with methylprednisolone 1 mg/kg was prescribed for the early phase of ARDS, but was discontinued twice, on April 23 and April 28, because of the high viral load and a low CD4 count. An undetectable (Ct value of >35) viral load of H7N9 after 15 days' treatment with NIs was observed on May 2, 2017, and the CD4 count increased gradually with the decreased viral load. We restarted systemic steroid use with methylprednisolone 2 mg/kg, then tapered to 0.5 mg/kg to reduce the risk of ARDS-related pulmonary fibrosis; however, the patient's chest X-ray still revealed unresolved pneumonia (Figure 1C). ECMO and invasive mechanical ventilation were used for 10 and 31 days, respectively. The NI treatment was discontinued 5 days after confirmation of the undetectable (Ct value of >35) viral load of H7N9. Chest X-ray after removal of the endotracheal tube revealed resolved infiltration at the right middle lobe and severe left lung fibrosis (Figure 1D and 1E). Non-invasive ventilator was then used for mild respiratory distress. The patient had a low oxy-

gen demand and was discharged successfully on May 31, 2014. The follow-up chest CT revealed persistent left lung fibrosis (Figure 1F).

Discussion

Steroids are not recommended for patients with viral infection. In this case, we used the increase in the number of CD4 lymphocytes to detect restoration of the immune system, and used steroids when the CD4 lymphocytes count was close to 200/cumm. This result implied that the CD4 T lymphocyte count could be a guide for steroid treatment in patients with influenza pneumonia and ARDS.

Early use of steroid in patients affected by influenza A infection was associated with an increased risk of superinfection [4]. Brun-Buisson et al. evaluated 208 patients with severe H1N1 infections and ARDS in a multicenter study in France. Early steroid therapy (less than 3 days of mechanical ventilator use) was associated with increased mortality. Steroid use was also associated with bacterial pneumonia and prolonged mechanical ventilation [5]. Yang, J. W. *et al*. conducted a meta-analysis that indicated early steroid use was strongly associated with mortality, compared to no steroid use. It is possible that very early corticosteroid administration enhances persistent viral replication and limits host defenses against future infections [6]. Persistence of viral shedding, as a predisposing factor and a complication of influenza infection, has recently been associated with a poorer outcome and longer hospital stay [7]. In an animal study, the use of corticosteroids was associated with slow decreases in viral load and poor outcomes [8]. However, no completed randomized controlled trials of adjunctive corticosteroid therapy for the treatment of influenza were found. Data specific to mortality are of a very low quality. As a result, there was insufficient evidence in the Cochrane review to determine the effectiveness of corticosteroids for patients with influenza [9]. Delaney, J. W. *et al*. conducted an observational cohort study that revealed no significant association between corticosteroids and mortality, after adjusting for time-dependent differences [10].

In the cellular response to influenza virus infection, recall of memory CD4 T cells offers considerable advantages in immune responses. Seasonal influenza provides memory CD4 T cells that can cross-reactively recognize H7 hemagglutinin (HA)–derived peptides. Richards, K. A. *et al*. suggested that previous exposure of humans to seasonal influenza can position them to respond to avian H7N9 [11]. Cross-reactive CD8+ T lymphocytes memory-generated after a prior encounter with seasonal or pandemic influenza A virus, or by a CD8+ T lymphocytes-directed vaccine, could potentially limit the severity of an H7N9 pandemic [12]. Infection outcomes in known H7N9 cases revealed some of the differences that were influenced by the extent of cross-reactive CD8+ T lymphocytes memory [12]. T-cell exhaustion in chronic infection such as human immunodeficiency virus, hepatitis B virus, and hepatitis C virus has been found before. In acute infection, the immune response will be dampened and the development of memory T cells will be found after pathogen clearance [13]. Recent studies on the Zika virus found CD4+ T cells were required to induce a humoral response and local control of the Zika virus burden in mice infected intravaginally [14]. This phenomenon may exist in other virus infections and can be used in vaccine development. Systemic steroid treatment in the early phase of influenza virus

infection potentially suppresses the immune response to influenza virus in peripheral blood mononuclear cells (polymorphonuclear leukocytes, lymphocytes, and monocytes), and has the potential to delay viral clearance.

In our case, the gradually increased CD4 T lymphocyte count accompanied with the slowly decreasing H7N9 viral load may indicate that the immune system has been restored. Although there is no strong evidence of the anti-inflammatory effects of steroid use in influenza infection, early use of steroid may increase the mortality rate and the incidence of hospital-acquired infection. The CD4 T lymphocyte count may be a guide to steroid treatment in critically ill patients.

There is no clear benefit to late steroid use in patients with ARDS. In a meta-analysis, Yang JW et al. found that early corticosteroid use was associated with more mortality than no corticosteroid use. However, subgroup analysis of the corticosteroid effect based on early and late use could not be performed due to insufficient data [7]. Late steroid use may enhance the resolution of lung consolidation caused by virus infection-induced organizing pneumonia.

The current strategy and timing of systemic corticosteroid use in the treatment of severe influenza pneumonia are controversial. In the case of H7N9, we discontinued systemic steroid use in the early phase of ARDS to avoid delaying viral clearance by the immune system in patients presenting with lymphopenia and a high viral load. After restoration of the immune system and completion of viral clearance, systemic steroid treatment was restarted based on the increased CD4 lymphocyte count and undetectable H7N9 viral load.

We suggest that the CD4 T lymphocyte count could be a guide for steroid treatment in patients with influenza pneumonia and ARDS. The findings in our study might help intensivists formulate a timely therapeutic strategy for systemic corticosteroid use in similarly severe patients with influenza infection and emerging viral infections.

H7N9 virus infection continues to have a high mortality rate (34%) [15], which is associated with severe pneumonia and multiorgan dysfunction. In our case, severe pulmonary fibrosis was found on the chest X-ray and chest CT (Figure 1F) after disease control. The timing of steroid use so as to avoid ARDS-related pulmonary fibrosis is still undetermined, as seen in previous studies. Further prospective studies are needed to determine the best timing for steroid use in patient with ARDS.

Disclosure Statement

Appropriate written informed consent was obtained for publication of this case report and accompanying images.

References

1. Povoa P, Salluh JI. What is the role of steroids in pneumonia therapy? Curr Opin Infect Dis 2012; 25(2): 199-204.
2. Lucas SJ, Barry DW, Kind P. Antibody production and protection against influenza virus in immunodeficient mice. Infect Immn 1978;20: 115-9.
3. Reiss CS and Burakoff SJ. Specificity of the helper T cell for the cytolytic T lymphocyte response to influenza viruses. J Exp Med 1981;154: 541
4. Martin-Loeches I, Lisboa T, Rhodes A, *et al*. Use of early corticosteroid therapy on ICU admission in patients affected by severe pandemic (H1N1)v influenza A infection. Intensive Care Med 2011; 37(2): 272-83.
5. Brun-Buisson C, Richard JC, Mercat A, *et al*. Early corticosteroids in severe influenza A/H1N1 pneumonia and acute respiratory distress syndrome. Am J Respir Crit

Care Med 2011; 183(9): 1200-6.

6. Yang JW, Fan LC, Miao XY, *et al*. Corticosteroids for the treatment of human infection with influenza virus: a systematic review and meta-analysis. Clin Microbiol Infect 2015; 21(10): 956-63.
7. Nedel WL, Nora DG, Salluh JI, *et al*. Corticosteroids for severe influenza pneumonia: A critical appraisal. World J Crit Care Med 2016; 5(1): 89-95.
8. Zhang AJ, To KK, Li C, *et al*. Leptin mediates the pathogenesis of severe 2009 pandemic influenza A(H1N1) infection associated with cytokine dysregulation in mice with diet-induced obesity. J Infect Dis 2013; 207(8): 1270-80.
9. Rodrigo C, Leonardi-Bee J, Nguyen-Van-Tam J, *et al*. Corticosteroids as adjunctive therapy in the treatment of influenza. Cochrane Database Syst Rev 2016; 3: CD010406.
10. Delaney JW, Pinto R, Long J, *et al*. The influence of corticosteroid treatment on the outcome of influenza A(H1N1pdm09)-related critical illness. Crit Care 2016; 20: 75.
11. Richards KA, Nayak J, Chaves FA, *et al*. Seasonal influenza can poise hosts for CD4 T-cell immunity to H7N9 avian influenza. J Infect Dis 2015; 212(1): 86-94.
12. Quinones-Parra S, Grant E, Loh L, *et al*. Preexisting CD8+ T-cell immunity to the H7N9 influenza A virus varies across ethnicities. Proc Natl Acad Sci USA 2014; 111(3): 1049-54.
13. Saeidi, A., Zandi K, Cheok YY, *et al*. T-cell exhaustion in chronic infections: reversing the state of exhaustion and reinvigorating optimal protective immune responses. Front Immunol 2018; 9: 2569.
14. Elong Ngono, A., Young MP, Bunz M, *et al*. CD4+ T cells promote humoral immunity and viral control during Zika virus infection. PLoS Pathog 2019; 15(1): e1007474.
15. Li Q, Zhou L, Zhou M, *et al*. Epidemiology of human infections with avian influenza A(H7N9) virus in China. N Engl J Med 2014; 370(6): 520-32.

Huge Chest Wall and Intrathoracic Desmoid Tumor: A Case Report and Literature Review

Lai-Man Mok[1], Yu-Chao Yu[1], Mei-Lin Chan[1], Wen-Chien Huang[1]

A desmoid tumor of the chest wall is rare. It is a slow-growing soft-tissue tumor, but also has an infiltrative growth tendency, which leads to a higher risk of local recurrence. However, it seldom metastasizes due to its benign nature. Surgical excision is the mainstay of treatment for the disease. Chest wall reconstruction would be necessary when a huge defect or loss of stability result from resection. Thus, a large tumor size and some specific locations would increase surgical complexity, which might lead to morbidity and mortality. We reported a 52-year-old female with a huge intrathoracic tumor. The patient underwent surgery for tumor removal via a sternotomy. The wound was extended to the left lower neck since the tumor was located at the left apex and close to the great vessels. Final pathology proved the diagnosis of a desmoid tumor of the chest wall and thoracic cavity. We presented the clinical features of the desmoid tumor and a discussion on management options and considerations. ***(Thorac Med 2022; 37: 27-32)***

Key words: desmoid tumor, fibromatosis, intrathoracic tumor, chest wall tumor, surgical treatment

Introduction

Desmoid tumors (DTs), also known as desmoids-type fibromatosis or aggressive fibromatosis, are a slow-growing fibroblastic proliferation that develops in the deep soft tissues. They are characterized by infiltrative growth and a tendency towards local recurrence but thye do not metastasize. These benign tumors account for approximately 0.03 % of all neoplasms [1]. DTs can develop anywhere in the body, but usually arise from the abdomen [4]. DTs of the chest wall are rare and represent only 10% to 20% of all fibromatoses, while intrathoracic locations are even rarer. There is no recommended standard approach for DTs currently, and surgical excision remains the first-line treatment [5-6]. In this case, a 52-year-old woman presented with chest wall and intrathoracic DT, and underwent surgical resection at our hospital. No local regional recurrence was noted during the OPD follow-up.

Case Report

A 52-year-old female presented to the emergency room due to left chest pain for 1 hour, which radiated to her back and was ag-

[1]Division of Thoracic Surgery, Department of Surgery, Mackay Memorial Hospital, Taipei, Taiwan
Address reprint requests to: Dr. Lai-Man Mok, Division of Thoracic Surgery, Department of Surgery, Mackay Memorial Hospital, No. 92, Chung-Shan North Road, Taipei 104, Taiwan

gravated by breathing. Chest X-ray (CXR with a posteroanterior view) revealed a large opacity at the left upper lung field and blunting of the left costophrenic angle (Figure 1). A computed tomography (CT) scan of the thorax with contrast showed an iso-dense and inhomogeneous mass, about 17 cm x 15 cm x 9 cm in size, in the left thoracic cavity, with close contact to the mediastinum and left upper lung but no obvious vessel or rib invasion (Figure 2). CT-guided biopsy of the mass reported a spindle cell tumor. Follow-up CT at 3 months showed that the tumor size remained the same. Later, the patient underwent tumor excision using a median sternotomy approach, with the incision extending to the lower neck and left sternocleidomastoid

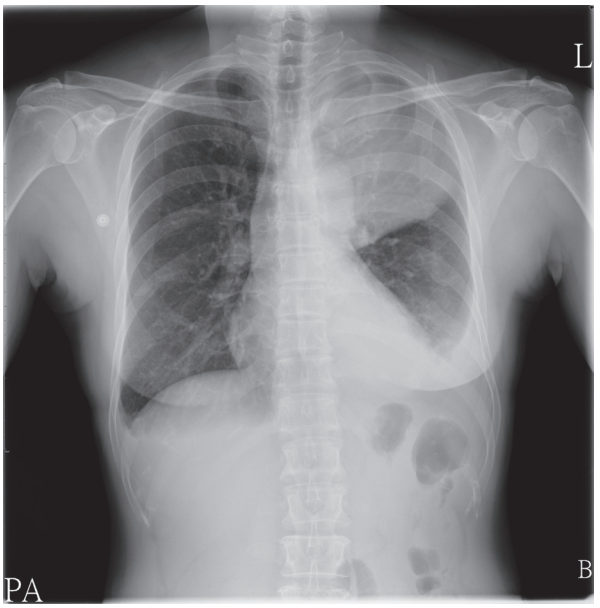

Fig. 1. CXR showed a left upper lung opacity and blunting of the costophrenic angle.

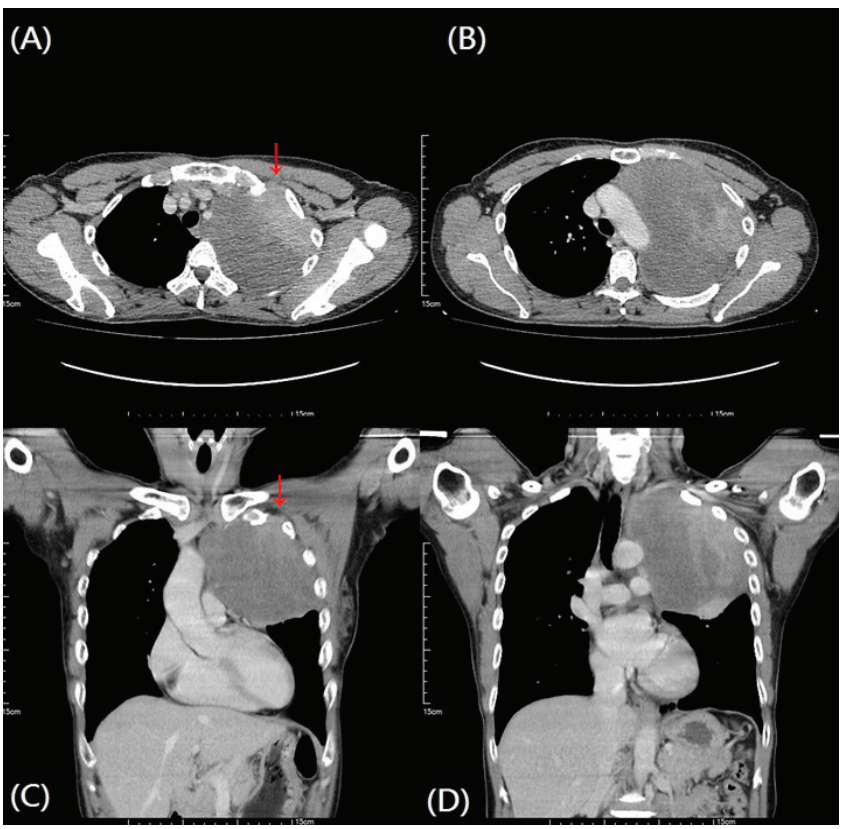

Fig. 2. A CT scan of the thorax with contrast, (A)(B)axial view and (C)(D) coronal view, showing an inhomogeneous soft tissue density mass, about 17 cm x 15 cm x 9 cm in size, in the left thoracic cavity, with close contact with the mediastinum and left upper lung, but no obvious vessel or rib invasion. The red arrow shows that the tumor invaded the 1st intercostal muscle.

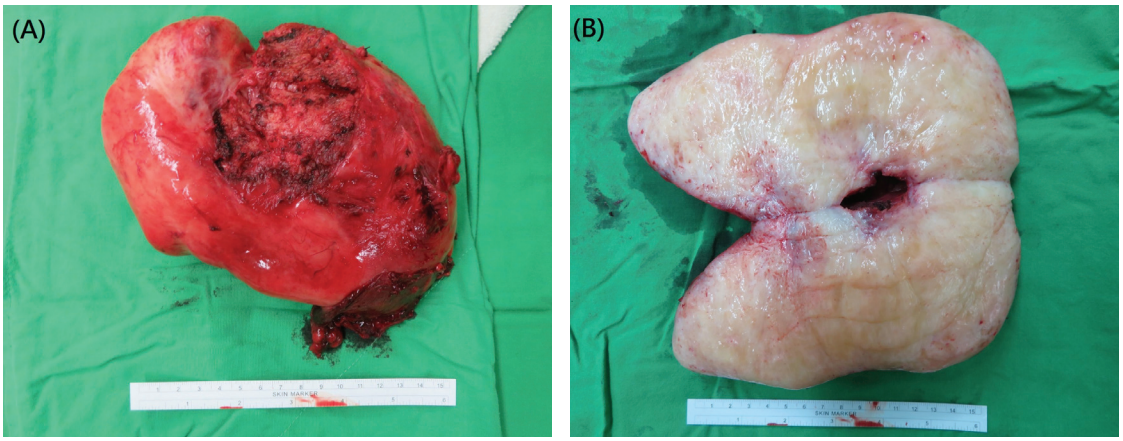

Fig. 3. A large, elastic, and homogenous tumor about 20 cm x 12cm x 10cm in size, arising from the left 1st intercostal muscle.

muscle – intraoperative findings confirmed a large, elastic, and homogenous tumor about 20 cm x 12cm x 10cm in size, arising from the left 1st intercostal muscle (Figure 3). We resected the tumor and the intercostal muscle beneath it. The phrenic nerve was encased and was resected along with the tumor. The adjacent vessels, lungs, and ribs were well preserved without injury. The patient was discharged home under stable condition on postoperative day 10.

Pathology(Figure 4) was compatible with desmoid-type fibromatosis, and the immunohistochemical (ICH) stain showed spindle cells with beta-catenin(patchy+), SMA(focal+), desmin(-), CD34(-), STAT-6(equivocal), MUC4(-) and S100(-). The patient was generally well and had a regular follow-up at the OPD. Left diaphragm eventration could be seen from the post-operative CXR (Figure 5). A CT scan at 4 months after surgery reported no evidence of local-regional recurrence (Figure 6).

Discussion

Desmoid tumors (DTs) are benign, deep-seated monoclonal myofibroblastic neoplasms that grow slowly in an infiltrative manner, and arise from musculoaponeurotic stromal elements. While most DTs arise sporadically, a minority of DTs is associated with Gardner syndrome. These tumors develop slightly more commonly in women than in men, with a peak age during their 30s. On the molecular level, DTs are characterized by mutations in the β-catenin gene, CTNNB1, or the adenomatous polyposis coli gene, APC [1-2], which result in an accumulation of β-catenin [4]. The etiology of these tumors is still unclear but likely multifactorial. Genetic factors, endocrine system, and trauma all play a role [1]. The ICH stain of our patient's tumor was positive for beta-catenin, indicating that the patient had gene mutations in CTNNB1 or APC. According to previous studies, DTs often arise from the abdominal wall of a pregnant woman, a post-surgical scar, or the site of previous trauma [1, 4]. Our patient was not pregnant at the moment but could have suffered a chest trauma before. We supposed that both genetic factors and trauma led to the occurrence of the desmoid tumor in the chest wall of our patient.

The clinical course of DTs varies – spontaneous regression, long-lasting stable disease or disease progression can occur [1-4]. DTs

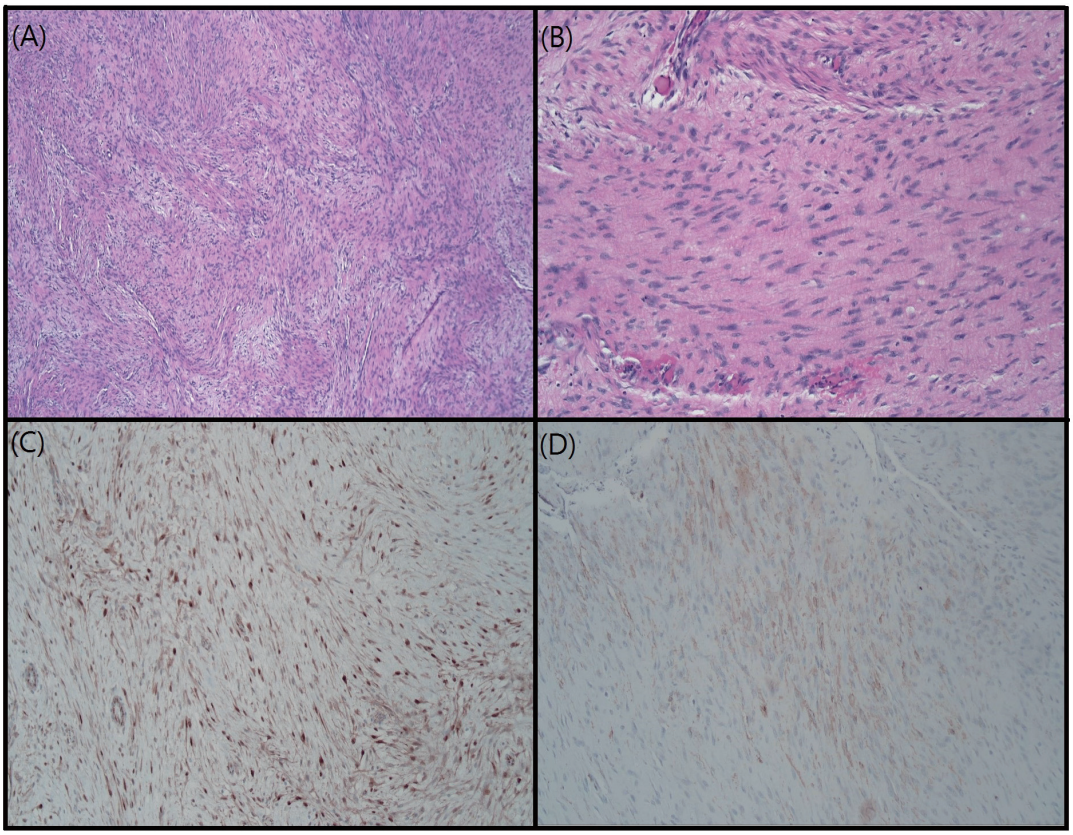

Fig. 4. Histologic patterns of the desmoid tumor (A, H&E x100). The tumor is composed of elongated, slender, spindle-shaped cells, forming long bundles, set in a collagenous stroma (B, H&E x200). The IHC stain showed positive for beta-catenin (C) and SMA(D, brownish area).

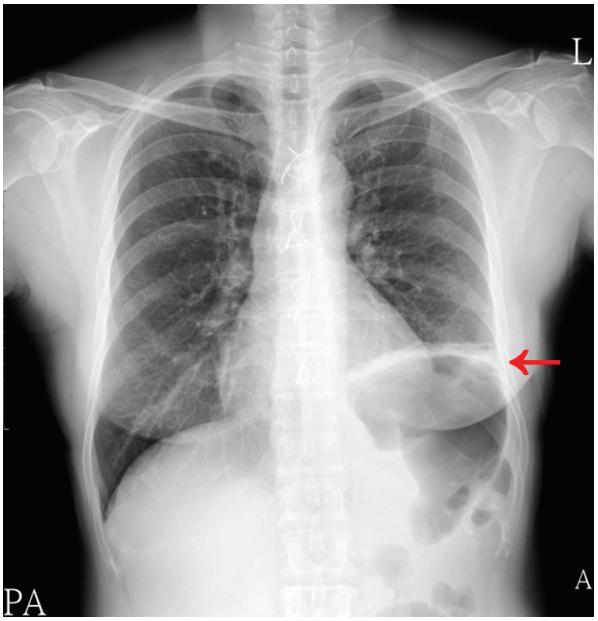

Fig. 5. Postoperative CXR showing left diaphragm eventration (red arrow).

are usually asymptomatic. However, pain and symptoms resulting from direct compression of local anatomical structures may occur when the DTs grow large [2, 4].

Both CT and magnetic resonance imaging (MRI) are valuable modalities for the diagnosis and assessment of DT. The image presented in the CT scan of our patient was compatible with previous reports [2], and showed a tumor with iso-dense to skeletal muscle and inhomogeneous foci corresponding to collagenous or myxoid areas. Other studies have mentioned that MRI is considered the gold standard radiological tool for diagnosing, assessing, and monitoring, since specific MRI features have been described and have been correlated to disease status. During disease progression,

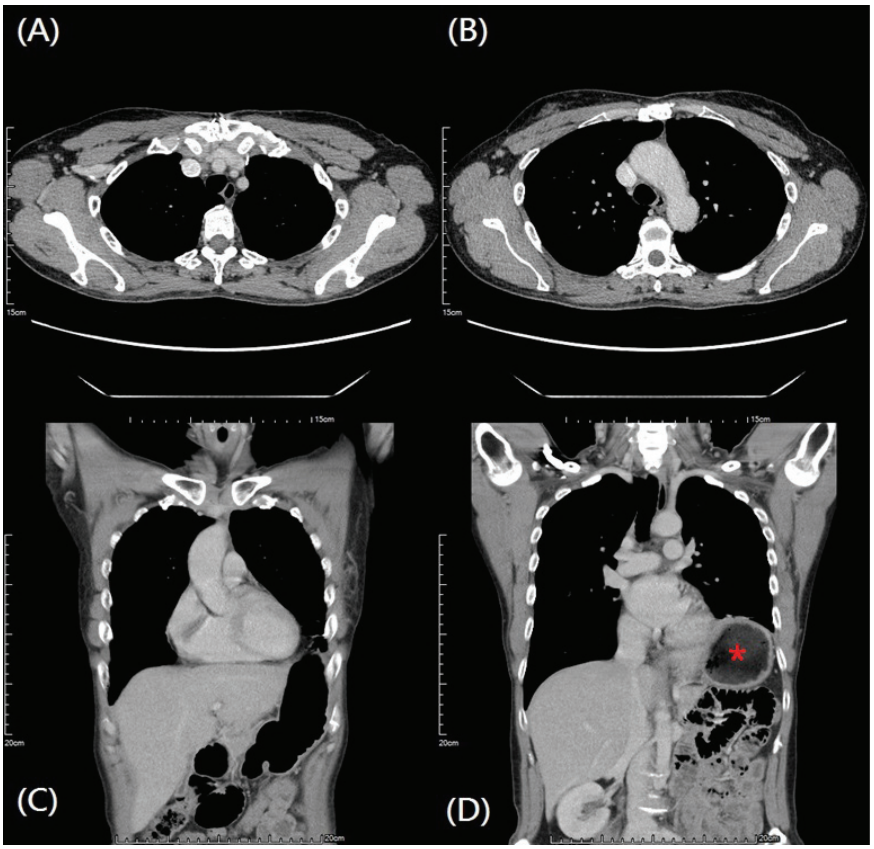

Fig. 6. CT at 4 months after surgery, (A)(B) axial view, and (C)(D) coronal view, showed no local recurrence, but revealed left diaphragm eventration (Red star: stomach).

DTs are heterogeneously hyperintense (corresponding to high cellularity) on T2W images, with bands of low signal (corresponding to the dense assemblies of collagen bundles) in all sequences. Spontaneous regression and dimensional response to treatment are often predicted by altered characteristics (compared with the baseline image) on MRI, such as – increased T2 hypo-intensity and decreased enhancement [2, 4]. We did not arrange MRI for tumor evaluation before the operation, but we can use MRI sensitivity to detect disease progression, regression, or recurrence. The choice of modality of can be made during follow – up [4].

At present, there is no standard treatment protocol for DTs. For asymptomatic diseases, close observation (watchful waiting) is an acceptable strategy because of the benign behavior of the tumors, including long term disease stabilization and spontaneous regression. For symptomatic diseases, several treatment modalities have been used by clinicians, including surgical resection, radiotherapy(RT), hormone therapy, non-steroidal anti-inflammatory drugs, chemotherapy, and targeted agents [1- 2, 4]. If technically feasible, surgical resection is the main treatment for resectable tumors. Some studies have indicated that a negative margin might be significant in terms of a lower local recurrence rate but not in terms of overall survival [11]. A 2 to 4 cm margin generally is accepted, according to a previous study [5].

DTs of the chest wall usually present in the form of a tumor of various sizes, but often

are large. In the literature, the average tumor size was 8.75cm (varying from 2 to 21 cm) [5-6, 11]. Because of the propensity of the tumor to invade vital structures, managing large DTs involving the chest region is always a challenge for thoracic surgeons [8]. Patients may still have functional loss or cosmetic deformity even after reconstruction for large chest wall defects. Vital organs and great vessels may be invaded or be adjacent to the tumor making the operation more complicated. A complex procedure carries a complication rate of up to 25%. Pneumonia or wound infection may occur and cause subsequent morbidity or mortality [11]. Meticulous considerations about the benefits and risks of a complex surgery must be taken. The overall surgical strategy should be to attempt complete removal using function-preserving approaches to minimize major morbidity [8-11]. In this case, we did remove the huge tumor, including the tumor itself and the appressed 1st intercostal muscle, without a chest wall resection. This was possibly an R0/R1 resection, although the pathologist reported that the resection margin could not be evaluated due to fragmented tissue.

The overall local recurrence rate of chest wall DTs after surgical excision is reported to be from 16% to 75% in different studies [5-6, 8-11]. RT as an adjuvant therapy after surgery can lower local recurrence, especially in patients with positive margins. It can also be used as a neoadjuvant treatment to increase the respectability rate. However, the use of RT alone to control a gross disease is not feasible because of the high rates of radiation-related complications [1-4, 6-8, 10]. Some studies reported that other pharmacology treatments can also be benefit of patients as an adjuvant treatment after the surgery or for those who are unfit for surgery. [1-4, 9, 11]. For our patient, adjuvant RT or other pharmacology treatments could be considered if there was a concern about an inadequate resection margin or a high risk of local recurrence. Otherwise, postoperative close follow-up is also appropriate.

References

1. Escobar C, R. Munker R, J.O. Thomas JO, *et al*. Update on desmoid tumors. Ann Oncol 2012; 23 (3): 562-9.
2. Fiore M, MacNeill A, Gronchi A, *et al*. Desmoid-type fibromatosis evolving treatment standards. Surg Oncol Clin N Am 2016; 25: 803–26.
3. Eastley NC, Hennig IM, Esler CP, *et al*. Nationwide trends in the current management of desmoid (aggressive) fibromatosis. Clin Oncol 2015; 27 (6): 362-8.
4. Eastley N, McCulloch T, Esler C, *et al*. Extra-abdominal desmoid fibromatosis: A review of management, current guidance and unanswered questions. ESJO 2016; 42(7): 1071-83.
5. Agrawal R, Choudhary P, Goel AK, *et al*. Large chest wall fibromatosis with challenging treatment plan. J Cancer Metas Treat 2017; 3: 139-43.
6. Zehani-Kassar A, Ayadi-Kaddour A, Marghli A, *et al*. Desmoid-type chest wall fibromatosis. A six-case series. Orthopaed & Traumatol: Surg Res 2011; 97: 102-7.
7. Guadagolo BA, Zagars GK, Ballo MT, *et al*. Long-term outcomes for desmoid tumors treated with radiation therapy. Int-J-Rad Oncol Biol-Phys- 2008; 71(2): 441-7.
8. Abbas AE, Deschamps C, Cassivi SD, *et al*. Chest wall desmoid tumors: results of surgical intervention. Ann Thorac Surg 2004; 78: 1219-23.
9. Cates JMM, Stricker TP.Surgical resection margins in desmoid-type fibromatosis. Am J Surg Pathol 2014; 38: 1707-14.
10. Mullen JT, DeLaney TF, Kobayashi WK, V. Desmoid tumor: analysis of prognostic factors and outcomes in a surgical series. Ann Surg Oncol 2012; 19: 4028-35.
11. Mátrai Z, Tóth L, Szentirmay Z, *et al*. Sporadic desmoid tumors of the chest: long-term follow-up of 28 multimodally treated patients. Eur J Cardio-thorac Surg 2011; 40(5): 1170-6.

Intralobar Pulmonary Sequestration with an Aberrant Feeding Artery Arising from the Celiac Trunk – A Case Report and Literature Review

Cheng-Hao Chuang[1], Chih-Hung Cheng[1], Yu-Chen Tsai[1], Ming-Ju Tsai[1,2], Jen-Yu Hung[1,2]

Pulmonary sequestration is an uncommon hereditary pulmonary anomaly that is classified into intralobar and extralobar types, based on whether it is coated with an independent visceral pleura. In patients with the intralobar type, there is abnormal communication with the normal respiratory tract, which easily leads to bacterial infection with clinical symptoms. We report a 25-year-old man who presented with pneumonia in the left lower lung. Tracing back his history, no systemic disease or risk factor for immunodeficiency was present, but he had repeatedly developed pneumonia in the left lower lung. Although his condition improved with antibiotic treatment, the follow-up chest radiograph showed slow improvement of the consolidation in the left lower lung. Computed tomography of the chest with contrast enhancement disclosed intralobar pulmonary sequestration with an aberrant feeding artery arising from the celiac trunk. The patient was treated surgically and had an uneventful recovery without further infection. Our case highlights the importance of an awareness of the presence of anatomical anomalies when physicians treat patients with recurrent pneumonia. ***(Thorac Med 2022; 37: 33-37)***

Key words: pulmonary sequestration; celiac trunk; intralobar type

Introduction

Pulmonary sequestration is a cause of respiratory distress and recurrent lower respiratory tract infection in children. It also affects adults, although rarely. Lack of familiarity often leads to this potentially treatable disease not being recognized. In our case, a 25-year-old man who had suffered from repeated episodes of left lower lobe pneumonia for many years presented with pulmonary sequestration and an aberrant feeding artery arising from the celiac trunk.

Case Report

A 25-year-old man with no known systemic

[1]Division of Pulmonary and Critical Care Medicine, Kaohsiung Medical University Hospital, [2]School of Medicine, College of Medicine, Kaohsiung Medical University, Kaohsiung, Taiwan
Address reprint requests to: Dr. Jen-Yu Hung, Division of Pulmonary and Critical Care Medicine, Department of Internal Medicine, Kaohsiung Medical University Hospital, Kaohsiung Medical University, No.100, Tzyou 1st Road, Kaohsiung 807, Taiwan

disease had had several episodes of pneumonia since childhood (Figure 1A). He presented to the emergency department due to intermittent spiking fever with copious sputum for 3 days. Mild chest tightness with pleuritic chest pain aggravated by deep inspiration was also noted. Physical examination disclosed coarse crackles in the bilateral lower lung fields, especially on the left side. Chest radiograph (Figure 1B, C) revealed a consolidated lesion in the left lower lung field with an elevated left hemidiaphragm. Leukocytosis with a left shift (12,580 leukocytes/μL with 15% band forms) and a markedly increased C-reactive protein level (377 mg/L) were noted. Computed tomography (CT) of the chest without contrast enhancement revealed consolidation with air-bronchogram and multiple scattered tiny calcifications in the left lower lobe, while bronchoscopy showed mucosal swelling with a narrowed orifice of the superior segment of the left lower lobe bronchus. The clinical condition improved with antibiotic treatment; however, while the patient was being followed up with chest radiographs in the out-

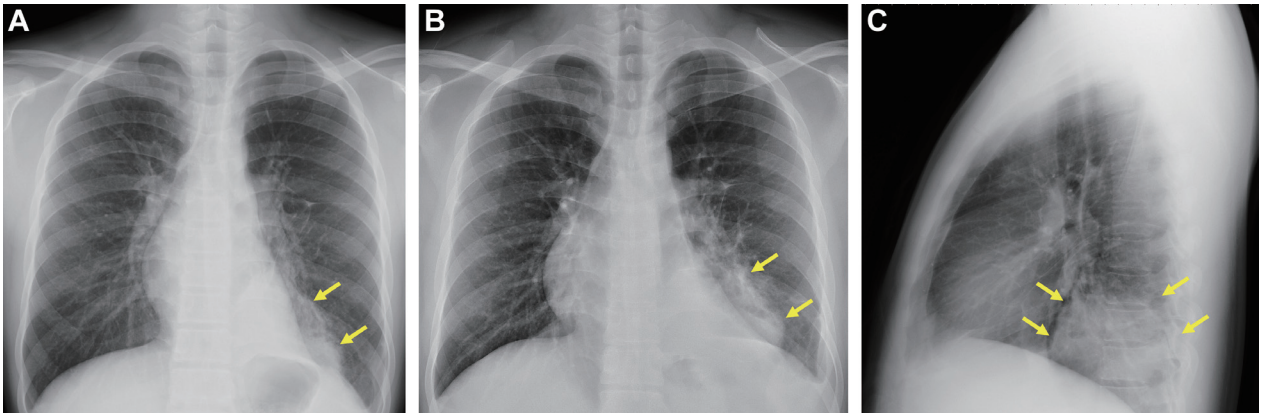

Fig. 1. Chest radiographs revealed repeated pneumonia in the left lower lobe (LLL) (arrows). (A) Chest radiograph on the occasion of LLL pneumonia 10 years prior to this admission. (B,C) The posteroanterior (B) and lateral (C) chest radiographs taken on the most recent admission showed LLL pneumonia.

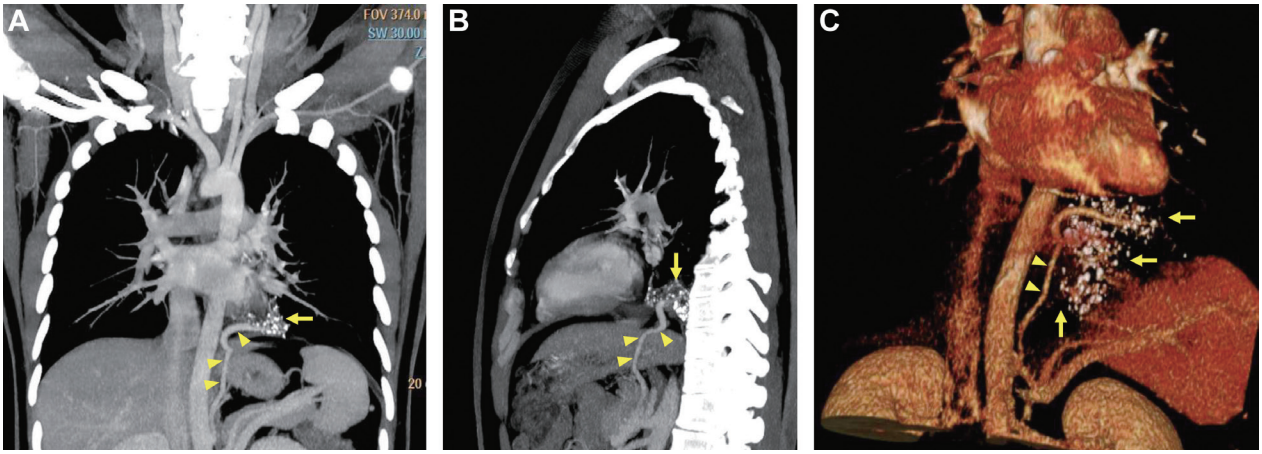

Fig. 2. Computed tomography (CT) of the chest with contrast enhancement disclosed intralobar pulmonary sequestration in the left lower lobe (arrows) with an aberrant feeding artery (arrowheads) arising from the celiac trunk. (A) Coronal view; (B) sagittal view; (C) reconstruction CT angiography.

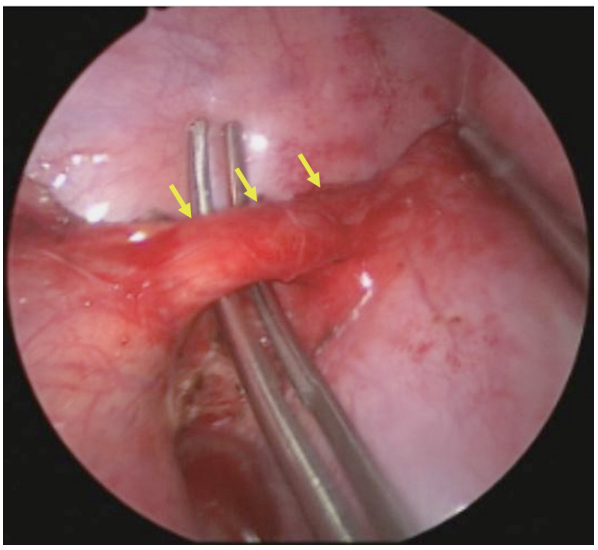

Fig. 3. Feeding artery (arrows) from the celiac trunk is identified and isolated intraoperatively.

patient department, slow resolution of the pulmonary consolidation was noted. The follow-up CT with contrast enhancement (Figure 2) disclosed pulmonary sequestration in the left lower lobe with an aberrant feeding artery originating from the celiac trunk. Surgical intervention was performed successfully, and a feeding artery from the celiac trunk was identified intra-operatively (Figure 3). Pathological examination confirmed the diagnosis of an intralobar type of sequestration (Figure 4). The patient had an uneventful recovery and no recurrent pneumonia was noted after the surgery.

Discussion

Pulmonary sequestration is a rare congenital broncho-pulmonary malformation comprising 0.15~6.4% of all congenital lung diseases, and is usually diagnosed during a prenatal evaluation or the perinatal period [1]. The main characteristics of pulmonary sequestration include a non-functioning lung mass without normal connection to the bronchopulmonary tree

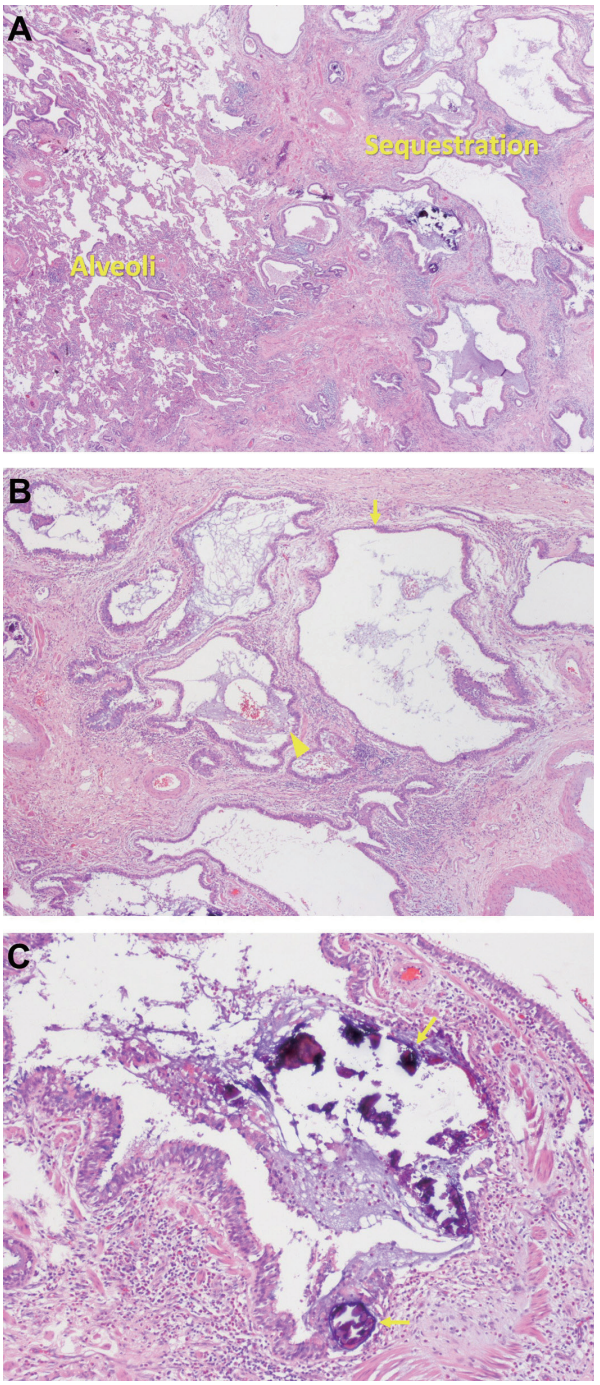

Fig. 4. Microscopy of the surgical specimen with hematoxylin and eosin stain ((A) magnification × 20; (B) magnification × 40; (C) magnification × 200) revealed: (A) No separating visceral pleura between the normal alveoli and the diseased sequestration part, which was compatible with an intralobar type of pulmonary sequestration. (B) Enlarged air-space with cystic dilatation (arrows) and mucus plugging (arrowheads). (C) Retention of mucus and calcification (arrows) in the enlarged air-spaces.

and an aberrant arterial supply from systemic circulation. The condition was first described by Huber in 1777, and the term "sequestration" was introduced by Price in 1946 [2]. An embryonic developmental error is the most acceptable mechanism to explain the spectrum of pathological findings in pulmonary sequestration. At 3 to 8 weeks of gestation, the normal primitive bronchial tree begins to develop and then bifurcates into right and left lung buds, followed by branching of the bronchial trees and the differentiation of epithelial cells into ciliated, goblet, and basal cells. Then, definitive lobes form and continue to mature. Meanwhile, if a supernumerary lung bud emerges during this period, arising caudal to the normal lung bud and migrating caudally, pulmonary sequestration develops [3].

Pulmonary sequestration is classified into 2 types: an intralobar type, which is embedded in the normal lung tissue without its own visceral pleura, and an extralobar type, which is surrounded by its own visceral pleura and is separated from the normal lung completely. Detailed history-taking including the perinatal condition and associated congenital anomalies plus a physical examination are always the cornerstones of a correct diagnosis [4]. In adults, the most common symptom of pulmonary sequestration is coughing, followed by recurrent respiratory tract infection, hemoptysis, chest discomfort, and dyspnea. Though rare, chronic high-output heart failure related to left-to-right shunt may be a presenting complication. An anomalous connection to normal ventilated bronchi or the lung parenchyma usually exists in the intralobar type, and this serves as an entry for bacteria, resulting in a higher risk of pulmonary infection than for the extralobar type. Recurrent pneumonia in the affected lobe since childhood, as in our case, is therefore the typical manifestation leading to the diagnosis of an intralobar type. Pulmonary sequestration might have several manifestations on chest CT, including consolidation with or without cyst, bronchiectasis, and cavitation. The intralobar type may also show focal hyperlucency, related to gas entrance from the normal lung and air-trapping, whereas the extralobar type does not. In our case, the chest CT revealed focal consolidation due to an active infectious process and multiple calcifications related to previously repeated infections. On pathological examination, the diseased part was sharply demarcated from normal lung tissue by abnormal parenchyma with an enlarged airspace, wall thickening, dilated airway structure, mucus plugging, and even microcystic changes. Absence of its own visceral pleura under microscopy confirmed the diagnosis of an intralobar type [5-6].

The posterior basal segment of the left lower lobe is the predominant site of intralobar pulmonary sequestration, and accounts for 56-73% of cases, as reported in several retrospective case series. The arterial supply of the sequestration comes mostly from the thoracic (54%) and abdominal (23%) aortas, and only a minor proportion of cases have a feeding artery originating from the celiac trunk (11%). In our case, a feeding artery from the celiac trunk was identified on the CT image pre-operatively and confirmed intra-operatively. The venous return pathway is hard to define in about half of the cases, as in our patient, but drainage to the pulmonary vein (30%), azygos vein (8%), and left atrium (8%) has been identified in other cases [5-6].

Definitive treatment is strongly recommended for symptomatic patients, and surgical excision serves as the first choice. Angiography

with embolization can be considered in cases of small-sized sequestration supplied by a single artery. Emerging evidence supports treatment via trans-arterial embolization (TAE) with occluding material or a mechanical device. This shows great potential in terms of treatment efficacy and has a low risk of procedure-related complications, compared to surgical intervention. However, several problems related to TAE should be addressed, including inadequate embolization, a high recurrence rate (25~47%), risk of embolization material migration, contrast exposure, and local hematoma that might lead to limb ischemia. The lack of a tissue specimen for pathological confirmation and the exclusion of a superimposed malignancy are major concerns. After considering these issues, our patient choose surgical intervention. The optimal treatment modality for asymptomatic patients remains controversial. Surgical intervention is generally accepted due to its curative efficacy and low complication rate. However, whether asymptomatic pulmonary sequestration in an adult really carries a higher risk of developing pulmonary infection is debatable [7].

In our case, the history of recurrent pneumonia in an otherwise healthy young male attracted our attention. He had no known underlying disease that might have contributed to his recurrent pneumonia, such as respiratory system diseases, immune insufficiency, malignancy, gastrointestinal diseases, or malfunctioning of the cardiovascular or neurological systems. The repeated pneumonia involving his left lower lung suggested a possible anatomical anomaly. CT without enhancement revealed only a consolidated lesion without obvious connection to the bronchial tree. The enhanced CT, which disclosed a feeding artery originating from the celiac trunk, confirmed the definitive diagnosis.

In summary, we reported an uncommon case of intralobar pulmonary sequestration with an aberrant feeding artery arising from the celiac trunk presenting with recurrent pneumonia. Physicians should consider the possible presence of anatomical anomalies when treating patients with recurrent pneumonia.

References

1. Savic B, Birtel FJ, Tholen W, *et al*. Lung sequestration: report of seven cases and review of 540 published cases. Thorax 1979; 34(1): 96-101.
2. Van Raemdonck D, De Boeck K, Devlieger H, *et al*. Pulmonary sequestration: a comparison between pediatric and adult patients. Eur J Cardiothorac Surg 2001; 19(4): 388-95.
3. Correia-Pinto J, Gonzaga S, Huang Y, *et al*. Congenital lung lesions--underlying molecular mechanisms. Semin Pediatr Surg 2010; 19(3): 171-9.
4. Geppert EF. Recurrent pneumonia. Chest 1990; 98(3): 739-45.
5. DeParedes CG, Pierce WS, Johnson DG, *et al*. Pulmonary sequestration in infants and children: a 20-year experience and review of the literature. J Pediatr Surg 1970; 5(2): 136-47.
6. Alsumrain M, Ryu JH. Pulmonary sequestration in adults: a retrospective review of resected and unresected cases. BMC Pulm Med 2018; 18(1): 97.
7. Borzelli A, Paladini A, Giurazza F, *et al*. Successful endovascular embolization of an intralobar pulmonary sequestration. Intervent Radiol 2017; 27: 13(1).

Diagnosing Mediastinal Metastatic Cholangiocarcinoma Using Eendobronchial Ultrasound-guided Transbronchial Needle Aspiration: A Case Report

Yi-Luen Shen[1], Ming-Huang Chen[2], Heng-Sheng Chao[1]

The diagnosis of a neoplasm in the gastrointestinal tract is usually based on pathologic examination via endoscopic biopsy or endoscopic ultrasound-guided fine-needle aspiration. However, tumor obstruction hinders the detailed tumor assessment and accuracy of endoscopic biopsies or endoscopic ultrasound-guided fine-needle aspiration. We report a rare case with an esophageal mass. While the obstruction prevented successful biopsy via the esophagus, endobronchial ultrasound-guided transbronchial fine-needle aspiration (EBUS-TBNA) was able to obtain adequate tissue samples by puncturing the tracheobronchial wall to the mass lesion outside the subcarinal area. Pathology disclosed adenocarcinoma that was CK7 positive. Based on the pathology and positron emission tomography findings, metastatic cholangiocarcinoma with esophageal metastasis was favored during the cancer multidisciplinary team discussion. EBUS-TBNA would be an effective method to obtain tissues in such situations. ***(Thorac Med 2022; 37: 38-42)***

Key words: endobronchial ultrasound; metastatic cholangiocarcinoma; esophageal neoplasm

Introduction

Real-time endobronchial ultrasound-guided transbronchial needle aspiration (EBUS-TBNA) provides simultaneous visualization and sampling accuracy. Compared with mediastinoscopy, video-assisted thoracoscopy and thoracotomy, EBUS-TBNA is safe and minimally invasive, and is the procedure of choice for mediastinal and lung tumors adjacent to the tracheobronchial trees. However, there are few available reports on the efficacy of EBUS-TBNA with regard to mediastinal lesions in patients with previous extra-pulmonary malignancies.

The mainstream diagnostic method for esophageal neoplasm is upper gastrointestinal endoscopy (UGIE) with biopsy, or alternatively,

[1]Department of Chest Medicine, Taipei Veterans General Hospital, Taipei, Taiwan, [2]Division of Medical Oncology, Department of Oncology, Taipei Veterans General Hospital, Taipei, Taiwan
Address reprint requests to: Dr. Heng-Sheng Chao, Division of General Chest Medicine, Department of Chest Medicine, Taipei Veterans General Hospital, Taipei, Taiwan No. 201, Sec. 2, Shih-Pai Rd., Beitou District, Taipei 11217, Taiwan, ROC

biopsy guided by endoscopic ultrasound (EUS). However, this could be technically challenging in the presence of tumor obstruction or external compression that hinders the detailed tumor assessment and accuracy of endoscopic biopsies. The risk of perforation is increased when performing EUS. In such circumstances, EBUS-TBNA via bronchoscopy could be an alternative tool to confirm the diagnosis when the lesion is adjacent to tracheobronchial trees. Here, we introduce a case with a mediastinal mass that was biopsied by EBUS-TBNA, after EUS had failed.

Case Report

A 66-year-old woman was admitted to our hospital because of a 3-month history of progressive swallowing difficulty. The symptom worsened with time, regardless of whether she was swallowing liquid or solid food. Her medical history was positive for hepatolithiasis, and she underwent cholecystectomy and hepatic segmentectomy 2 years ago. The patient had undergone percutaneous transhepatic cholangiography and drainage for unexplained obstructive jaundice about 4 months prior to this presentation.

On this occasion, computed tomography of the chest showed marked wall thickening of the esophagus, around 3.4 cm in length, at the level of the aortopulmonary window to the subcarinal area, with proximal esophageal dilatation. Increased soft tissue at the aortocaval space at the level of the celiac trunk and intrahepatic duct dilatation were still found with tube drainage. Upper gastrointestinal endoscopy revealed 2 submucosal nodules, 0.6-0.8 cm in diameter, at 27 cm from the incisor. Since the endoscope failed to pass through the esophageal stricture at the middle-third esophagus, EUS was applied, and disclosed an infiltrating lesion extending from the mucosa layer beyond the esophageal wall.

Biopsies of the mucosa were taken several times on. Endoscopic ultrasound-guided fine-needle aspiration (EUS-FNA) was not performed because of the proximity of the lesions to the descending aorta. The pathology of the esophageal ulceration disclosed atypical glands only. Whole-body positron emission tomography showed a hypermetabolic tumor with esophageal obstruction (SUV: 6.8), lymphadenopathy on the retroperitoneum and gastrohepatic ligament (SUV: 5.6), and several sites with focally increased uptake on the liver, compatible with cholangiocarcinoma (SUV: 15.1) (Figure 1A-B).

Intervention pulmonologists were consulted for further tissue biopsy. Flexible bronchoscopy revealed no endobronchial lesions. Endobronchial ultrasound (EBUS Convex Probe BF-UC260FS; Olympus; ultrasound processor EU-ME2; Olympus) showed lesions in the subcarinal area close to the proximal left main bronchus. The subcarinal mass was punctured 3 times with a 22-gauge dedicated needle (Vizishot NA-201SX-4022; Olympus) under real-time EBUS-TBNA guidance. Rapid on-site adequacy assessment (ROSE) by a cytology technician was performed. The duration of the procedure was 19 minutes. (Figure 1 C-D). The pathologic findings revealed blood clots mixed with clusters of well-differentiated tall columnar mucinous glandular cells, compatible with adenocarcinoma (immunoreactive for CK7+, and non-reactive for CK20, CDX-2, and TTF-1) (Figure 2A-B). We reviewed the clinical data and discussed this in a meeting of the cancer multidisciplinary team. The team

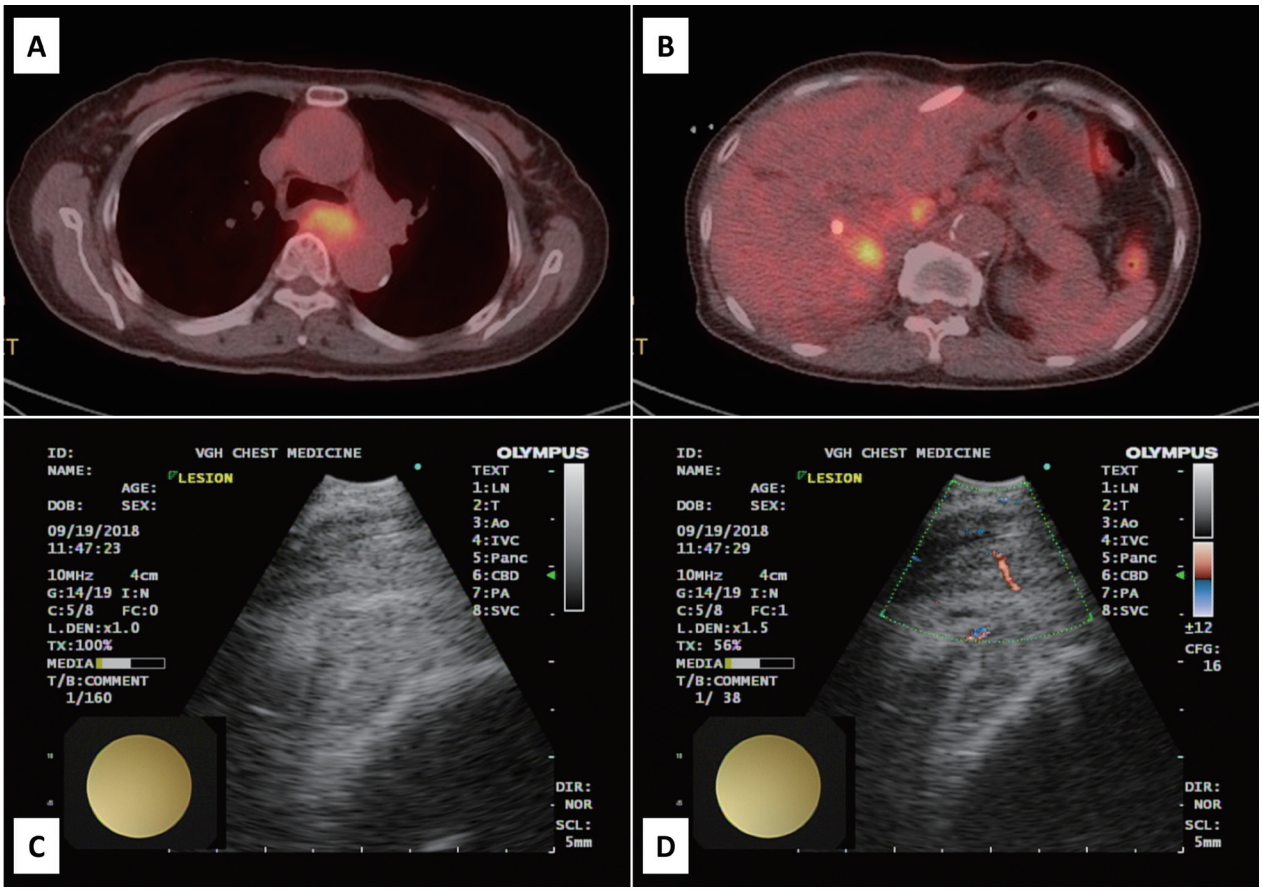

Fig. 1. F-18 FDG whole-body positron emission tomography/computed tomography imaging of endobronchial ultrasound and endobronchial ultrasound-guided transbronchial biopsy.
1A: Marked thickening of the esophageal wall, about 3.4 cm in length, from the aortopulmonary window to the subcarinal level with increased uptake. (SUV: 6.8) 1B: Several sites of focally increased uptake (SUV: 15.1) are noted on the liver. 1 C&D: Mass-like lesion with submucosal infiltration that was detected at the subcarinal level, confluent with the esophagus. Intralesional blood vessels were detected with color Doppler.

came to the conclusion that this was cholangiocarcinoma with multiple metastasis, including the esophagus, instead of primary esophageal cancer or lung cancer. The patient subsequently was referred to a medical oncologist. She received chemotherapy for advanced cholangiocarcinoma, and esophageal stenosis stenting for palliative purposes.

Discussion

Since its emergence, the use of EBUS has become a trend in minimally invasive mediastinal staging because of its range and safety, and that its outcomes and yield rate are comparable to those of other staging methods. Yasufuku et al. demonstrated that EBUS achieves similar outcomes with fewer complications in mediastinal staging of lung cancer than mediastinoscopy [1]. The concept of combined EBUS-TBNA and EUS-FNA in lung cancer staging is widely accepted, and provides the best care for selected patients [2-4]. Navani et al. reported that EBUS reduces the time to treatment decisions compared with conventional diagnosis and staging techniques. The post-hoc analysis also revealed

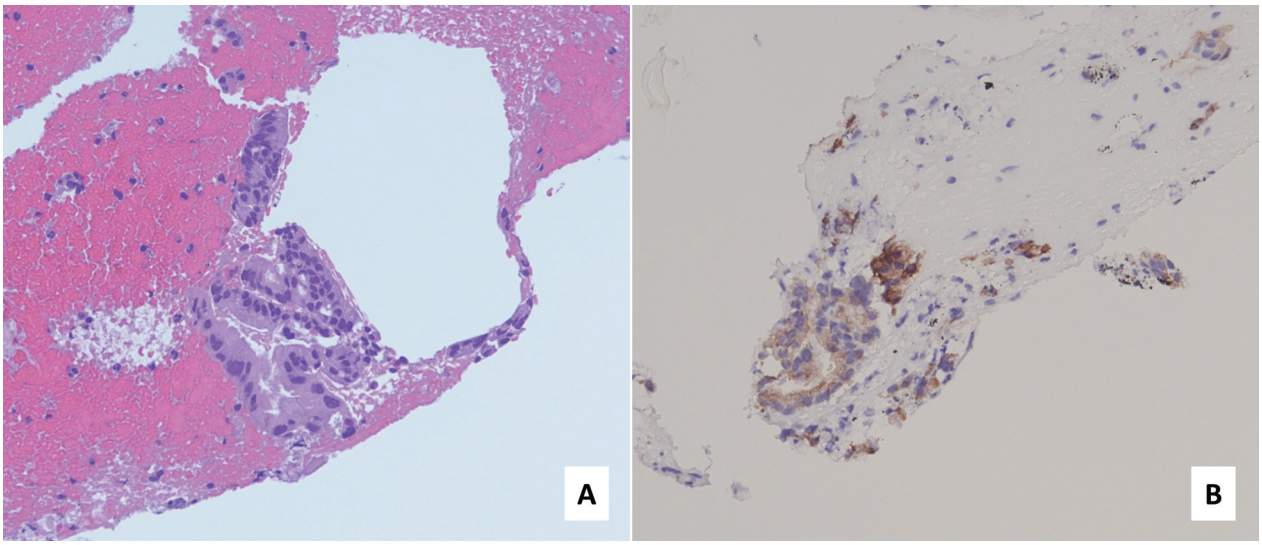

Fig. 2. Endobronchial ultrasound-guided transbronchial biopsy pathology findings.
2A: Blood clots admixed with clusters of well-differentiated tall columnar mucinous glandular cells. 2B: These glandular cells were immunoreactive for CK7.

superior survival rates in the EBUS group [5].

EBUS-TBNA for histopathological diagnosis of mediastinal extrapulmonary malignancy is anatomically reasonable, but there are few reports available concerning the efficacy of EBUS-TBNA with mediastinal lesions in patients with previous extrapulmonary malignancies. As for esophageal cancer, EBUS has played a secondary role to EUS in confirming local tumor extension (T stage) and lymph node status (N stage) in past studies. EBUS provides better accuracy for determining the depth and extent of tumor invasion into the airway wall, compared to conventional bronchoscopy [6]. The gold standard for diagnosing esophageal lesions is UGIE with biopsy, or alternatively, biopsy guided by EUS. But this is technically difficult when there is tumor obstruction or external compression obliterating the esophageal lumen. EBUS-TBNA can approach esophageal lesions above the subcarinal level in such cases, and collect representative specimens for diagnosis. It can be an alternative tool for those patients who failed to undergo UGIE or EUS-FNA. EBUS-TBNA for peritumoral lymph nodes is also helpful with regard to specimen contamination secondary to piercing the primary tumor. The combined EBUS-EUS staging procedure would improve precision in staging and can change the treatment plan in patients with esophageal cancer [7].

Cholangiocarcinoma arises from the epithelial cells of the intrahepatic and extrahepatic bile ducts. The clinical symptoms of extrahepatic or intrahepatic cholangiocarcinoma are usually different. Extrahepatic cholangiocarcinoma is prone to be symptomatic with biliary tract obstruction. Intrahepatic cholangiocarcinoma might be asymptomatic, or present right upper quadrant pain or constitutional symptoms. The liver is a common site of metastases, but this is rare compared to extra-abdominal metastasis. There are few reports on cholangiocarcinoma with esophageal metastasis. The possible mech-

anism of esophageal metastasis is lymphatic spreading. Tumor cells pass through efferent lymphatics retrogradely into the lamina propria of the esophagus, causing submucosal metastasis. [8] Histopathologic examination remains a gold standard for differentiating primary esophageal cancer from metastatic neoplasm.

To sum up, we reported a rare case of cholangiocarcinoma with esophageal metastasis that failed to be approached by EUS-FNA and endoscopic biopsies, and finally was diagnosed by EBUS-TBNA. This was a remarkable collaboration between gastroenterologists and pulmonologists. EBUS-TBNA via bronchoscopy can approach a lesion adjacent to tracheobronchial trees and confirm the diagnosis, even if the tumor originated from the gastrointestinal tract. Crosstalk between specialties, including thoracic surgeons, should be realized in the era of precision and personalized medicine.

References

1. Yasufuku K., Pierre A., Darling G, *et al*. A prospective controlled trial of endobronchial ultrasound-guided transbronchial needle aspiration compared with mediastinoscopy for mediastinal lymph node staging of lung cancer. J Thorac Cardiovasc Surg 2011; 142 1393-400.*e1*.
2. Navani N, Nankivell M, Lawrence DR, *et al*. Lung-BOOST trial investigators. Lung cancer diagnosis and staging with endobronchial ultrasound-guided transbronchial needle aspiration compared with conventional approaches: an open-label, pragmatic, randomised controlled trial. Lancet Respir Med 2015; 3: 282-9.
3. Herth FJ, Krasnik M, Kahn N, *et al*. Combined endoscopic-endobronchial ultrasound-guided fine-needle aspiration of mediastinal lymph nodes through a single bronchoscope in 150 patients with suspected lung cancer. Chest 2010; 138: 790-794.
4. Annema JT, van Meerbeeck JP, Rintoul RC, *et al*. Mediastinoscopy vs endosonography for mediastinal nodal staging of lung cancer: a randomized trial. JAMA 2010; 304(20): 2245-2252.
5. Vilmann P, Frost Clementsen P, Colella S, *et al*. Combined endobronchial and esophageal endosonography for the diagnosis and staging of lung cancer European Society of Gastrointestinal Endoscopy (ESGE) Guideline, in cooperation with the European Respiratory Society (ERS) and the European Society of Thoracic Surgeons (ESTS). Eur J Cardiothorac Surg 2015; 48(1): 1-15.
6. Wakamatsu T, Tsushima K, Yasuo M, *et al*. Usefulness of preoperative endobronchial ultrasound for airway invasion around the trachea: esophageal cancer and thyroid cancer. Respiration 2006; 73: 651-7.
7. Liberman M, Hanna N, Duranceau A, *et al*. Endobronchial ultrasonography added to endoscopic ultrasonography improves staging in esophageal cancer. Ann Thorac Surg 2013; 96(1): 232-236.
8. Sato T, Krier M, Kaltenbach T, *et al*. Cholangiocarcinoma metastasis to the esophagus. Endoscopy (2010); 42(S 02), E250-E250.

Occult Parathyroid Carcinoma Presenting with Right Hilar Lymph Node Metastasis – A Case Report

Yi-An Hsieh[1], Yi-Chen Yeh[2], Yong-Yang Liu[3]

Parathyroid carcinoma is the rarest endocrine malignancy, and treatment options are limited. In some cases, treatment may be postponed due to misdiagnosis or delayed diagnosis. Most patients present with insidious symptoms of hypercalcemia only. We report a 74-year-old woman with parathyroid carcinoma who had an atypical presentation on a sestamibi (MIBI) parathyroid scan, which showed negative uptake in the primary parathyroid lesion but positive uptake in the metastasized right hilar lymph node. The definitive diagnosis was reached with the assistance of endobronchial ultrasound-guided transbronchial needle aspiration (EBUS-TBNA) of the right hilar lymphadenopathy. This case report may serve to remind clinicians of the challenges and pitfalls in the diagnosis of occult parathyroid carcinoma and present an alternative approach to reaching a definite diagnosis via EBUS-TBNA. ***(Thorac Med 2022; 37: 43-50)***

Key words: parathyroid carcinoma, hypercalcemia, sestamibi (MIBI) parathyroid scan

Introduction

Parathyroid carcinoma is the rarest endocrine malignancy, and represents 1% of all cases of primary hyperparathyroidism [1]. It can be a genetic syndrome or, more commonly, exist as sporadic cases. Parathyroid cancer usually occurs in patients over 40 years old, with no predilection for sex or race [2]. It presents with a range of biochemical and clinical characteristics, but overall is considered to have an indolent evolution. Patients often present with hypercalcemia (>14 mg/dl) and related skeletal and renal complications [2-3]. Biochemical and clinical presentations are similar to benign parathyroid disease, and the definitive diagnosis is usually not recognized before surgery. Clues including local invasion or the presence of lymph node or distant organ metastases may prompt the suspicion of malignancy [4-5].

[1]Department of Chest Medicine, Taipei Veterans General Hospital, [2]Department of Pathology and Laboratory Medicine, Taipei Veterans General Hospital, [3]Division of Clinical Respiratory Physiology, Department of Chest Medicine, Taipei Veterans General Hospital
Address reprint requests to: Dr. Division of Clinical Respiratory Physiology, Department of Chest Medicine, Taipei Veterans General Hospital, No. 201, Sec. 2, Shipai Rd., Beitou Dist., Taipei City 112201, Taiwan (R.O.C.)

We report a patient who suffered from symptomatic hypercalcemia and enlargement of the right hilar lymph node that was proved to be metastatic carcinoma lymphadenopathy by endobronchial ultrasound-guided transbronchial needle aspiration (EBUS-TBNA). Parathyroid carcinoma was further identified by right subtotal parathyroidectomy and thyroid lobectomy. We present this case due to its rarity and challenges in diagnosis, and present an alternative approach to diagnosis via EBUS-TBNA of the intrathoracic lymphadenopathy.

Case Report

A 74-year-old female with a history of hypertension, hyperlipidemia, and type 2 diabetes mellitus was admitted for body weight loss of about 8 kgs in the most recent 2 weeks. She presented with polyuria, polydipsia, nausea, constipation, loss of appetite, muscle weakness, and severe fatigue. She denied dysphagia, abdominal pain, tarry stool, cough, night sweats, or fever. Before this admission, she could perform daily work independently. She was a non-smoker and denied a family history of multiple endocrine neoplasia (MEN) or other hereditary diseases. On physical examination, she was alert, but was clinically dehydrated with dry mucous membranes and reduced skin turgor. There was no palpable mass in her neck or abdomen. A chest X-ray showed right hilar enlargement (Figure 1). Laboratory investigations revealed severe hypercalcemia with a serum calcium level of 15.3 mg/dl (normal range, 8.4–10.6 mg/dl) and a decreased creatinine clearance of 8.9 ml/min (normal, >120 ml/min). The patient was admitted for further evaluation and treatment.

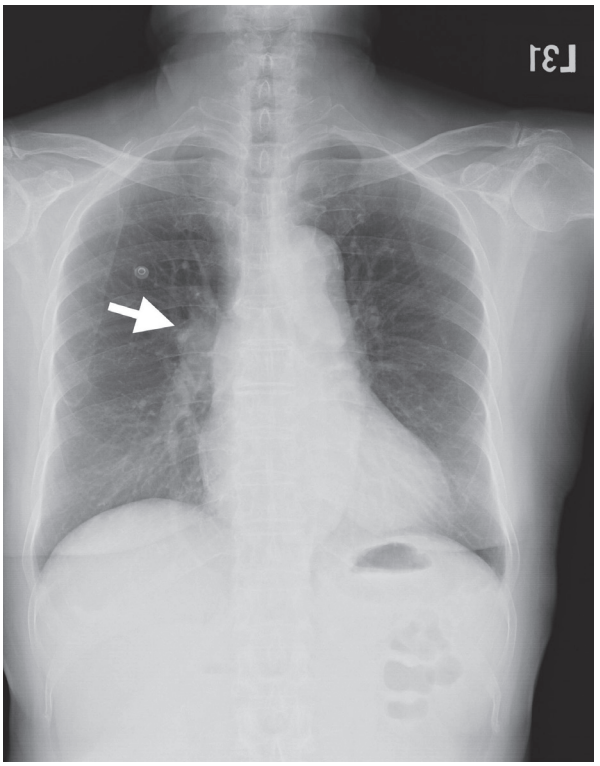

Fig. 1. CXR showing normal lung parenchyma with right hilar enlargement (arrow).

After admission, treatment with intensive hydration and calcitonin for hypercalcemia was begun. Malignancies prone to lung metastasis were surveyed, including thyroid, breast, and liver cancer, but there was nothing specific. However, an abnormality, a hypoechoic nodule 1.60 × 0.95 cm in size in the right retrothyroid region, was detected by neck ultrasound. Chest CT scanning showed enlarged lymph nodes in the right lower paratracheal space and right pulmonary hilum (Figure 2). The serum intact parathyroid hormone (iPTH) concentration was elevated to 431.3 pg/ml (normal range, 15.0–68.3 pg/ml). A 24-hour urine measurement showed an elevated total calcium level, and fractional excretion of calcium was 8.3% (normal, <2%).

These findings suggested a diagnosis of primary hyperparathyroidism. A further sestamibi

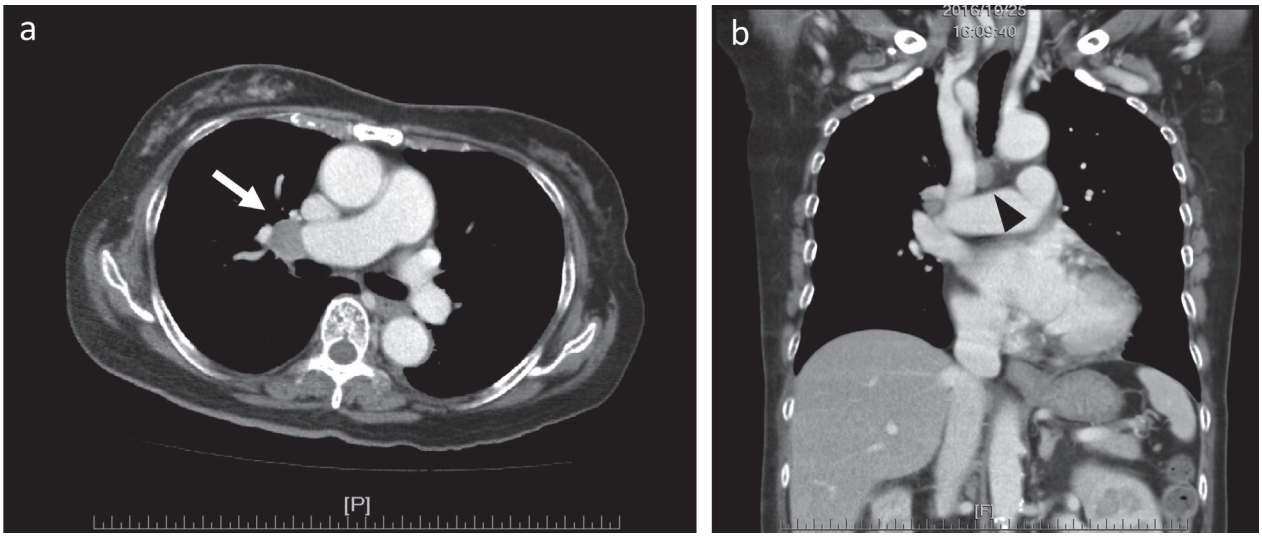

Fig. 2. Chest CT showing an enlarged lymph node at the right pulmonary hilum (a, arrow) and right lower paratracheal area (b, arrow head).

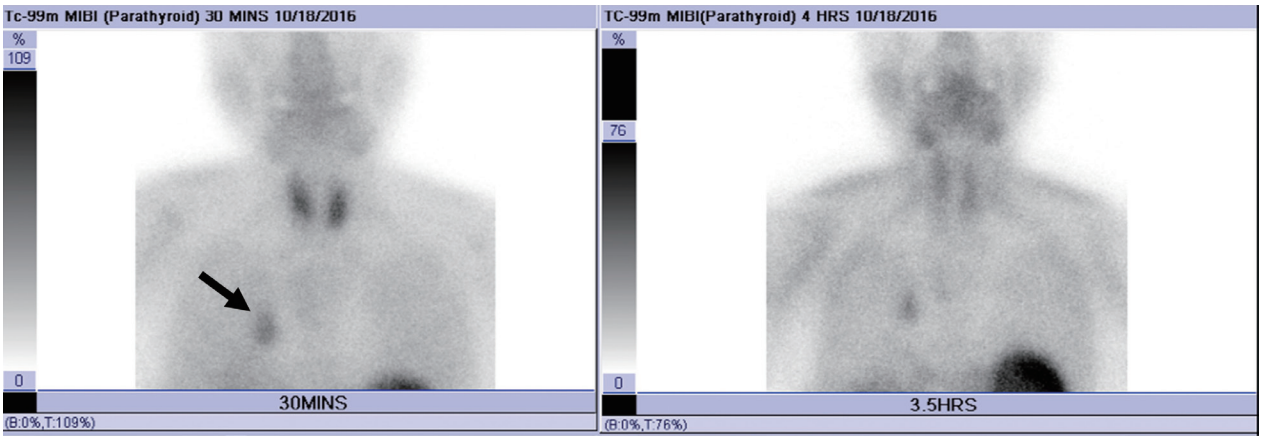

Fig. 3. MIBI scan showing negative uptake in the parathyroid region, but focally positive uptake around the right hilar area (arrow).

(MIBI) scan showed negative uptake in the parathyroid region, but a focally positive uptake around the right hilar area (Figure 3). Ectopic parathyroid adenoma was considered first, based on the disease prevalence. The differential diagnoses included parathyroid malignancy, tertiary hyperparathyroidism, and, though less likely, other malignancy.

EBUS-TBNA was performed on the enlarged right hilar lymph node at station 10R. Pathology indicated metastatic carcinoma, which mucicarmine staining and immunostains revealed to be positive for CK, GATA3, and PTH, and negative for CK7, CK20, TTF-1, ER, PR, and HER2. Further additional immunostains for chromogranin A and synaptophysin were diffusely positive, while SSTR2A and SSTR5 stains were negative. The Ki-67 index of the tumor cells was 15% (Figure 4).

The immunohistochemical profile favored a parathyroid tumor origin. However, whether it was a metastatic tumor from a parathyroid

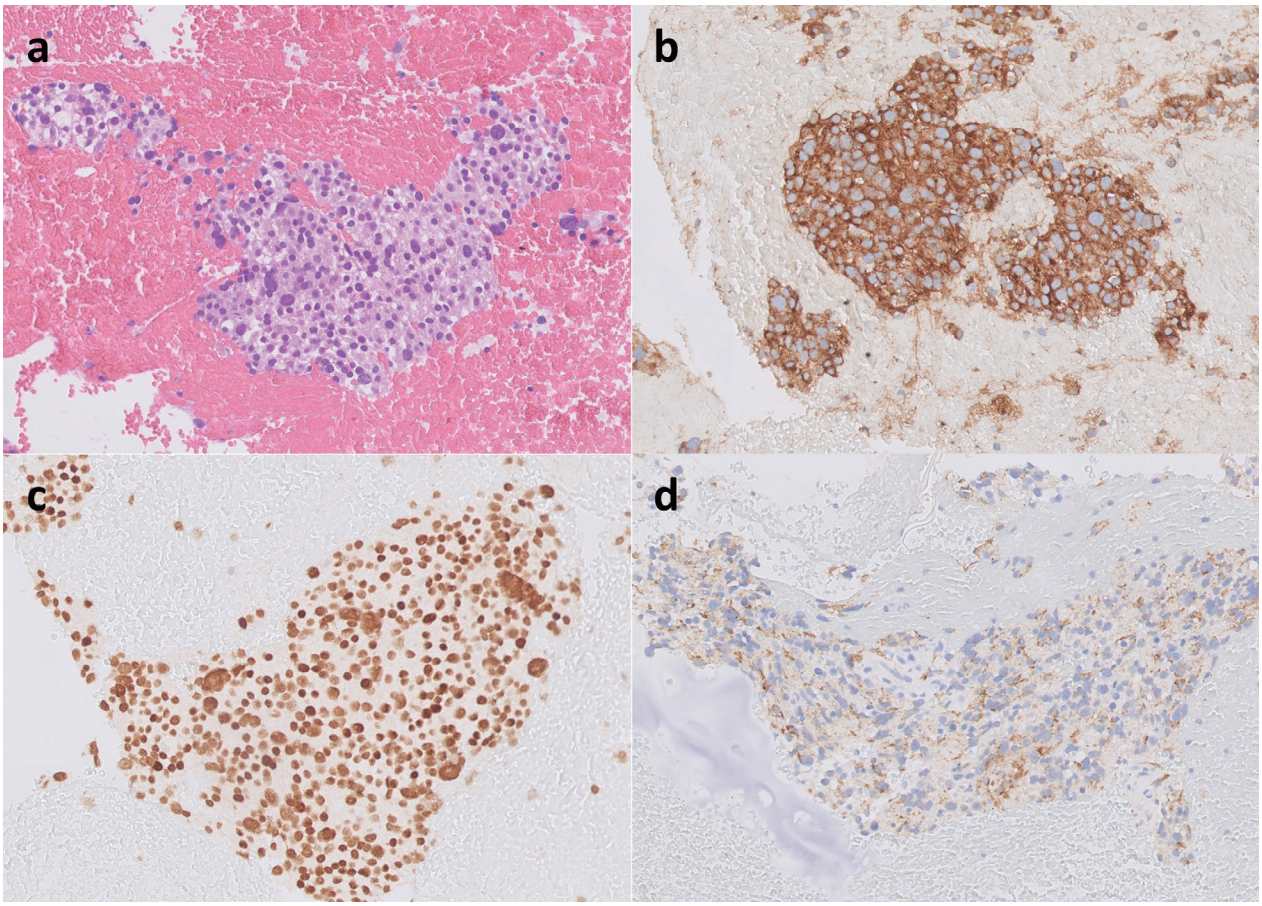

Fig. 4. Histopathologic examination of the biopsied tissue of the station 10R lymph node via EBUS-TBNA showing clusters of polygonal carcinoma cells with pleomorphic nuclei and clear-to-pink cytoplasm (a). The tumor cells were positive for chromogranin A (b), GATA3 (c), and PTH (d). (200X).

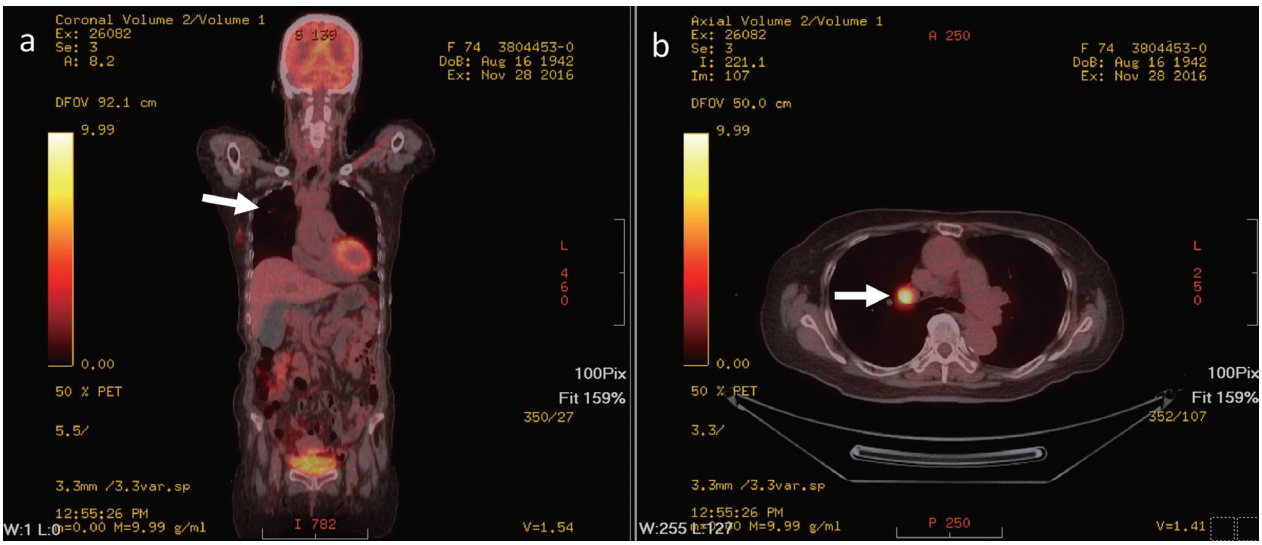

Fig. 5. Whole body PET/CT showed a 7 mm nodular lesion in the RUL (a) and an enlarged lymph node around 1.8 cm at station 10R (b).

neoplasm or ectopic parathyroid tissue could not be determined with this limited specimen. A whole-body PET/CT for further assessment showed an enlarged lymph node, around 1.8 cm, at station 10R, and a 7 mm nodular lesion in the right upper lobe (RUL) (Figure 5). After a combined conference with the general and chest surgeons, a right subtotal parathyroidectomy and thyroid lobectomy were performed. The pathology of the parathyroid tissue showed a high Ki67 labeling index (>30% at the most active area) and focal coagulative necrosis, which was compatible with the malignant nature of parathyroid tumors (Figure 6).

She subsequently underwent thoracoscopic wedge resection of the RUL nodule and radical mediastinal lymph node dissection. The pathology of the RUL nodule also showed metastatic parathyroid carcinoma. However, despite the almost complete removal of the primary tumor and metastatic lesions, the follow-up serum calcium level was still high. Therefore, the patient received combined chemotherapy with dacarbazine plus fluorouracil. The regimen was later shifted to etoposide plus cisplatin because of persistent progressive disease. The cancer status was still out of control and her condition deteriorated. Further palliative radiation therapy

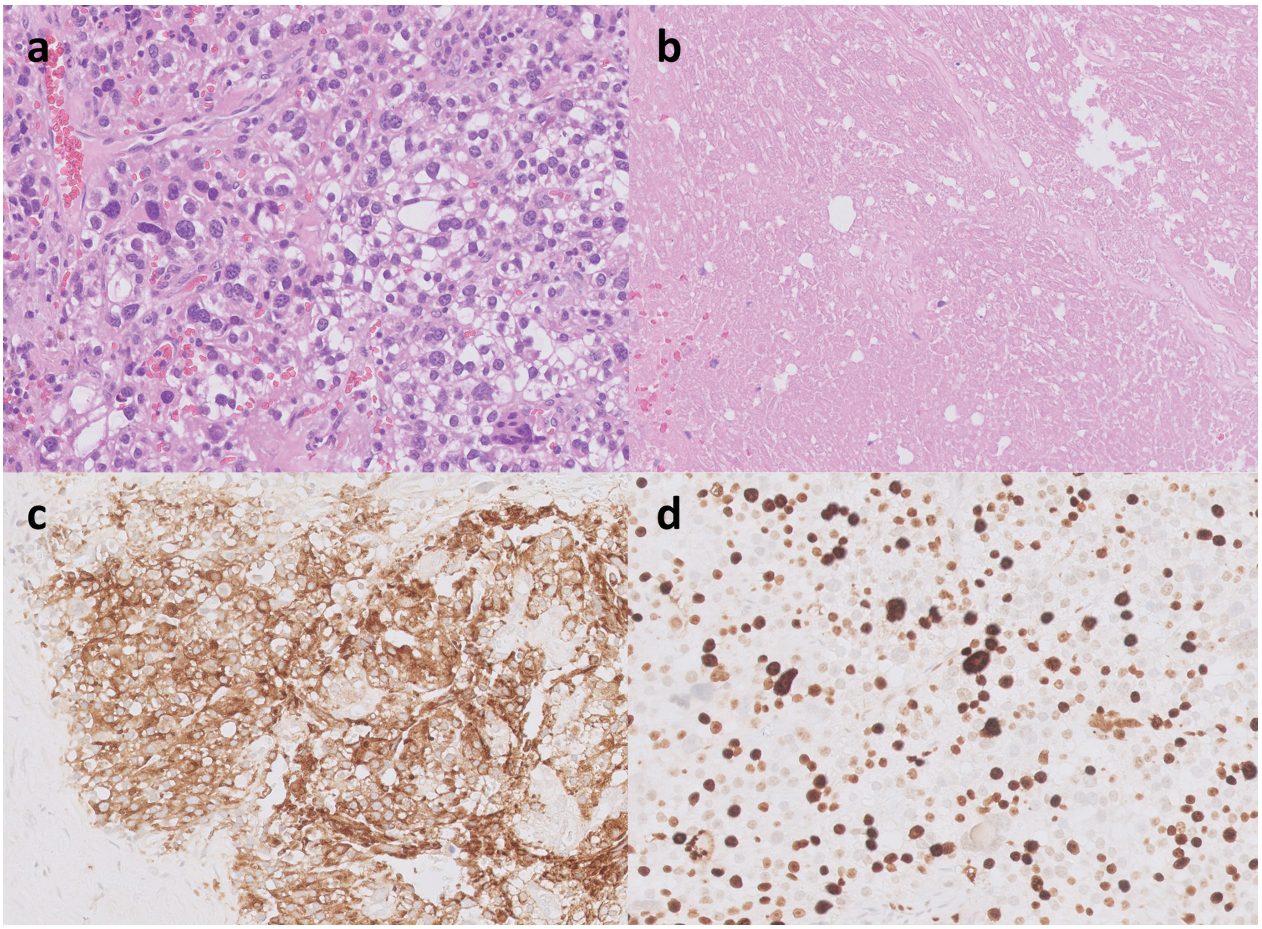

Fig. 5. Histopathologic examination of the resected right parathyroid tissue showing parathyroid carcinoma composed of clusters of polygonal carcinoma cells with pleomorphic nuclei and clear-to-pink cytoplasm (a). Tumor necrosis can be seen (b). The tumor cells were positive for PTH immunostain (c). A high Ki-67 labeling index is revealed by Ki-67 immunostaining (d). (200X).

was added. However, the patient died of tumor progression, severe hypercalcemia, and multiple organ failure.

Discussion

Parathyroid carcinoma is a rare endocrinologic malignancy, and the criteria for a definitive diagnostic are lacking. It may occur sporadically or in conjunction with familial hyperparathyroidism, hyperparathyroidism–jaw tumor syndrome, or multiple endocrine neoplasia (MEN) type 1 or 2A. It is usually silent and the only clues are a palpable neck mass (30–76%) and signs and symptoms of hypercalcemia [1, 3, 6]. Most patients present with severe hypercalcemia with total serum calcium levels greater than 13 mg/dL. Other clinical manifestations of parathyroid carcinoma include symptoms related to hypercalcemia, such as bone pain, weakness, pancreatitis, malaise, polyuria, polydipsia, nausea, and vomiting. In addition to hypercalcemia, the biochemical profile of a high PTH level might be another clue. Obscure symptoms, even in patients with moderate to severe hypercalcemia, are an obstacle to the diagnosis of parathyroid carcinoma.

Parathyroid carcinoma should be suspected in a patient with hypercalcemia and hyperparathyroidism or a neck mass. Serum calcium and PTH levels, neck ultrasonography and MIBI scan are required to reach a diagnosis. However, both neck ultrasonography and MIBI scan have low sensitivity in identifying parathyroid lesions. In contrast, MIBI scanning combined with sestamibi single-photon emission computed tomography (SPECT) carries greater sensitivity for localization of the lesions. The clinical presentations of parathyroid carcinoma are the same as those of parathyroid adenoma and parathyroid hyperplasia. Therefore, it is difficult to differentiate clinically between a benign and a malignant parathyroid tumor without pathological proof or image evidence of local invasion and distant metastasis. Moreover, parathyroid biopsy is of no value in establishing the diagnosis and should be avoided, as it poses a risk of tumor seeding into surrounding tissues, and parathyroid carcinoma is hard to distinguish from adenomas histologically. As such, parathyroid carcinoma is hard to diagnose before surgery.

The interesting aspect of the atypical presentation of our case is that the small parathyroid lesion detected by neck ultrasound showed a negative uptake on the MIBI scan, but focal MIBI uptake was obvious in the enlarged right hilar lymph node. Though the lung is a common site for metastases from parathyroid carcinoma [7-9], there has been only 1 case report with a similar presentation [10]. There are many factors that contribute to false-negative MIBI scans, including cell type [11] and increased expression of P-glycoprotein [12], though the evidence is weak.

We performed EBUS-TBNA of the station 10R lymphadenopathy which provided tissue proof of metastatic carcinoma from a parathyroid origin. EBUS-TBNA has emerged as a minimally invasive technique for the diagnosis of benign and malignant thoracic diseases, and is used mostly in lung cancer staging [13-14]. In our current case, we used this new and safe modality before operation as an effective diagnostic approach. Therefore, EBUS-TBNA may offer more information than parathyroid biopsy and render a diagnosis of parathyroid carcinoma prior to surgery.

The most effective treatment for parathyroid carcinoma is radical surgery with en bloc

resection of the lesion together with the ipsilateral thyroid, thyroid isthmus, lymph nodes, thymus, some of the neck muscles, and in some instances, the recurrent laryngeal nerve [1, 15]. Because patients with parathyroid cancer often suffer from hypercalcemia, preoperative medical intervention to control hypercalcemia is often required.

There are limited options for treatment if complete tumor removal cannot be performed [1, 16]. As recurrence and systemic metastases develop in up to 52% of patients with parathyroid carcinoma [17], total calcium and iPTH levels should be monitored frequently. Hypercalcemia may recur 3 months following surgery, so further systemic treatment may be required. However, treatment options for metastasis or refractory disease are limited. Dacarbazine has been proved to be effective for parathyroid carcinoma as single use or in combination with other chemotherapy regimens [18-19]. However, most chemotherapy and radiotherapy failed to show a significant positive effect on the course of the disease [1, 20].

Conclusion

In summary, parathyroid carcinoma is rare and poses a diagnostic challenge. Parathyroid carcinoma should always be kept in mind as a differential diagnosis of malignancy with hypercalcemia. Our case had the atypical presentation of parathyroid carcinoma with no MIBI uptake in the primary lesion and strong uptake in the right hilar lymph node. EBUS-TBNA might be a new and safe preoperative diagnostic approach for parathyroid carcinoma patients presenting with intrathoracic lymph node metastasis.

References

1. Shane E. Clinical review 122: Parathyroid carcinoma. J Clin Endocrinol Metab 2001; 86: 485-93.
2. Talat N, Schulte KM. Clinical presentation, staging and long-term evolution of parathyroid cancer. Ann Surg Oncol 2010; 17(8): 2156-74.
3. Wynne AG, van Heerden J, Carney JA, *et al*. Parathyroid carcinoma: clinical and pathologic features in 43 patients. Medicine (Baltimore) 1992; 71: 197-205.
4. Busaidy NL, Jimenez C, Habra MA, *et al*. Parathyroid carcinoma: a 22-year experience. Head Neck 2004; 26(8): 716.
5. Ippolito G, Palazzo FF, Sebag F, *et al*. Intraoperative diagnosis and treatment of parathyroid cancer and atypical parathyroid adenoma. Br J Surg 2007; 94(5): 566-70.
6. Chow E, Tsang RW, Brierley JD, *et al*l. Parathyroid carcinoma—the Princess Margaret Hospital experience. Int J Radiat Oncol Biol Phys 1998; 41: 569-72.
7. Shaha AR, Ferlito A, Rinaldo A. Distant methastasis from throid and parathyroid cancer. ORL J Otorhinolaryngol Relat Spec 2001; 63(4): 243-9.
8. Obara T, Okamoto T, Kanbe M, *et al*. Functioning parathroid carcinoma, clinicopathologic features and rational treatment. Semin Surg Oncol 1997; 13(2): 134-41.
9. Yamamoto T, Matsumura A. Clinical review 122: Parathyroid Carcinoma [Comment]. J Clin Endocrinol Metab 2001; 86(10): 5091.
10. Cengiz H , Baş S , Tütüncü Y. A rare case of parathyroid carcinoma, presented with functional lung metastases. Acta Medica Alanya 2018; 2(3): 206-9.
11. Bleier BS, LiVolsi VA, Chalian AA, *et al*. Technetium Tc 99m sestamibi sensitivity in oxyphil cell-dominant parathyroid adenomas. Arch Otolaryngol Head Neck Surg 2006; 132: 779-82.
12. Bhatnagar A1, Vezza PR, Bryan JA, *et al*. Technetium-99m-sestamibi parathyroid scintigraphy: effect of P-glycoprotein, histology and tumor size on detectability. J Nucl Med 1998; 39(9): 1617-20.
13. Lee HS, Lee GK, Lee HS, *et al*. Real-time endobronchial ultrasound-guided transbronchial needle aspiration in mediastinal staging of non-small cell lung cancer: how many aspirations per target lymph node station? Chest 2008; 134(2): 368-74.

14. Varela-Lema L, Fernandez-Villar A, Ruano-Ravina A. Effectiveness and safety of endobronchial ultrasound-transbronchial needle aspiration: a systematic review. Eur Respir J 2009; 33(5): 1156-64.
15. Sandelin K, Auer G, Bondeson L, *et al*. Prognostic factors in parathyroid cancer: a review of 95 cases. World J Surg 1992; 16: 724-31.
16. DasGupta R, Shetty S, Keshava NS, *et al*. Metastatic parathyroid carcinoma treated with radiofrequency ablation: a novel therapeutic modality. Australas Med J 2014; 7(9): 372–5.
17. Holmes EC, Morton DL, Ketcham AS. Parathyroid carcinoma: a collective review. Ann Surg 1969; 169(4): 631-40.
18. Bukowski R, Sheeler L, Cunningham J, *et al*. Successful combination chemotherapy for metastatic parathyroid carcinoma. Arch Intern Med 1984; 144(2): 399-400.
19. Calandra D, Chejfec G, Foy B, *et al*. Parathyroid carcinoma: Biochemical and pathologic response to DTIC. Surgery 1984; 96(6): 1132-7.
20. Schantz A, Castleman B. Parathyroid carcinoma: a study of 70 cases. Cancer1973; 31(3): 600-5.

Good Steroid Response in a Patient with Atypical Chronic Hypersensitivity Pneumonitis with Neutrophilia in the Bronchoalveolar Lavage Fluid: A Case Report and Literature Review

Shih-Yu Chen[1], Ping-Hung Kuo[1]

Chronic hypersensitivity pneumonitis (CHP) is a granulomatous disorder. The typical features of CHP include fibrotic changes in the upper or middle lungs on high resolution computed tomography (HRCT) and lymphocyte predominance in the bronchoalveolar lavage (BAL) fluid. In this report, we describe a middle-aged woman presenting with a chronic cough for 2 months. She had a history of exposure to ring-necked pheasants. HRCT revealed reticular opacities and fibrotic change in the bilateral basal lungs. The percentage of neutrophils in the BAL fluid was 75%. She underwent a video-assisted thoracoscopic surgery biopsy and the pathology was consistent with the typical findings of CHP. The patient's symptoms and diffusion capacity responded well to low-dose oral prednisolone treatment, and the follow-up HRCT revealed nearly total resolution of previous lesions. We also review the literature regarding the diagnostic and prognostic impact of atypical presentations of CHP. ***(Thorac Med 2022; 37: 51-57)***

Key words: chronic hypersensitivity pneumonitis (CHP), bronchoalveolar lavage (BAL), high resolution computed tomography (HRCT)

Introduction

Chronic hypersensitivity pneumonitis (CHP) is a granulomatous lung disease caused by recurrent environmental irritants [1]. There are currently no universal diagnostic criteria for CHP. The diagnosis often relies mainly on the incorporation of a history of symptoms, the recurrent clinical course, possible offending allergens, a bronchoalveolar lavage (BAL) survey, high-resolution computed tomography (HRCT) and histopathology [2-4].

In patients with CHP, the typical features of BAL are a high total cell yield with a lymphocyte predominance, a high ratio of CD8+/CD4+ T cells, and the presence of mast cells, plasma cells and foamy macrophages [3, 5, 6]. The pattern of upper lobe-predominant fibrotic changes

[1]Division of Pulmonary Medicine, Department of Internal Medicine National Taiwan University Hospital
Address reprint requests to: Dr. Ping-Hung Kuo, Division of Pulmonary Medicine, Department of Internal Medicine, National Taiwan University Hospital, No. 7, Chung-Shan South Road, Taipei 100, Taiwan

or the combination of fine nodular opacities and ground glass opacity are common HRCT findings and important for differentiating CHP from non-specific interstitial pneumonia or usual interstitial pneumonia [2, 3, 7].

Nevertheless, the diagnosis of CHP is often challenging because it may not always present with typical clinical manifestations. Here, we report a patient with steroid-responsive CHP presenting with atypical BAL and HRCT findings. We also review the literature on the diagnostic and prognostic impact of the atypical presentations of CHP.

Case Report

A 65-year-old woman presented to our chest outpatient clinic with a chronic cough with whitish sputum for more than 2 months. There was no associated hemoptysis, chest tightness, abdominal pain, myalgia, arthralgia, or skin eruptions. She had no previous systemic disease. She was treated as having community-acquired pneumonia at another hospital, but the symptoms persisted. She then was referred to this tertiary medical center for further survey.

On initial physical examination, her respiratory rate was 24/min, blood pressure 138/84 mmHg, heart rate 71/min, and body temperature 36o Celsius. Chest auscultation disclosed fine crackles in both lower lung fields. Other examinations, including the cardiovascular, abdominal, central nervous and musculoskeletal systems, were unremarkable. The hemogram and biochemistry and autoimmune profiles were within normal limits, except for an elevated ESR level, at 45 mm/hr (reference <20). The initial chest radiograph showed ill-defined opacities in the bilateral lower lung fields (Figure 1). The pulmonary function test showed a mildly impaired diffusion capacity (Table 1). Chest HRCT disclosed multiple subpleural patches and focal bronchiectasis in the bilateral lower lungs (Figure 2). The differential cytology of her BAL fluid revealed a neutrophil predominance (neutrophils 75%, macrophages 22.2%, epithelial cells 1.8%, and lymphocytes 1.0%). Cultures of the BAL fluid did not yield significant growth. She underwent a video-assisted thoracic surgical biopsy and the pathology from the right lower lung revealed centrilobular inflammation, peribronchiolar fibrosis and loosely-formed granuloma (Figure 3), suggesting a diagnosis of CHP.

A more detailed history-taking revealed that the patient had had a long-term heavy exposure history to ring-necked pheasants in her home environment. Avoidance of trigger exposure was suggested and prednisolone was adminis-

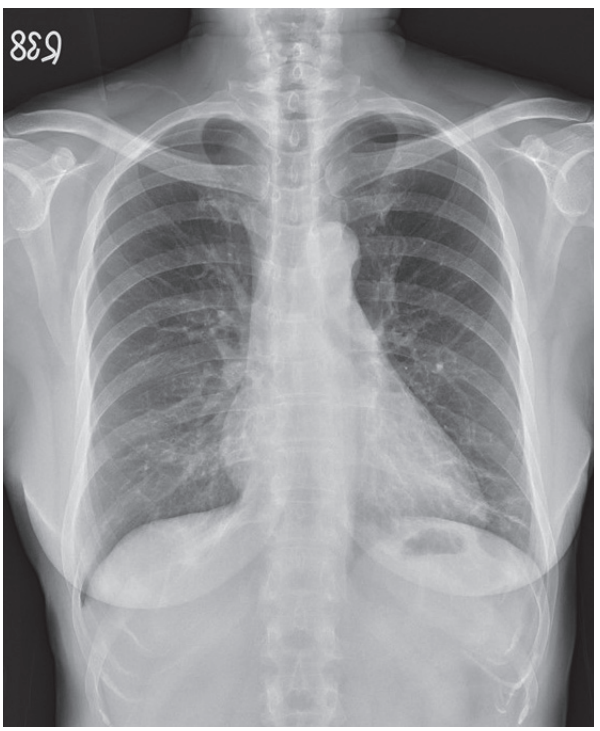

Fig. 1. Chest radiography showed ill-defined opacities in bilateral lower lung fields.

Table 1. Pulmonary Function Testing Before and After Steroid Therapy

	At presentation	4 months later (after steroid therapy)
FVC L (% of predicted)	2.81L (133.1%)	3.1L (144.5%)
FEV_1 L (% of predicted)	2.41L (144.7%)	2.69L (159%)
FEV_1/FVC	85.8%	86.8%
FEF 25%-75% L/S (% of predicted)	2.91 (137.3%)	3.19 (152%)
DLCO (ml/min/mmHg)	11.0 (72.3%)	15.1 (95.7%)
VA	3.81 (101.5%)	4.09 (107%)
DLCO/VA	2.90	3.68
Hb	12.4	12.4
DLCOcorr (ml/min/mmHg)	11.8 (77.6%)	16.2 (102.7%)

FVC: forced vital capacity; FEV1: forced expiratory volume in 1 second; FEF 25%-75%: forced expiratory flow at 25-75%; DLCO: diffusion capacity for carbon monoxide; VA: alveolar volume; Hb: hemoglobin; DLCOcorr: DLCO correction for hemoglobin;

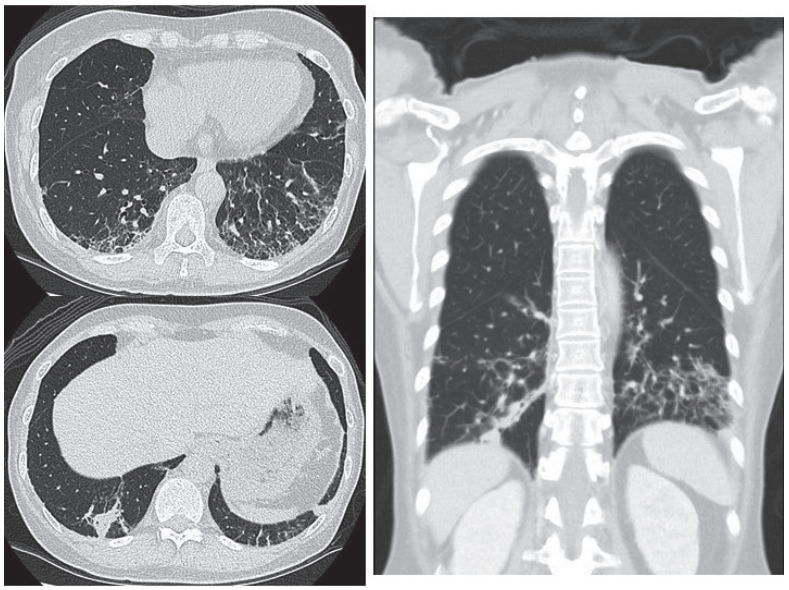

Fig. 2. HRCT on initial presentation showing bilateral basal lung reticular lesions, some consolidation, and traction bronchiectasis.

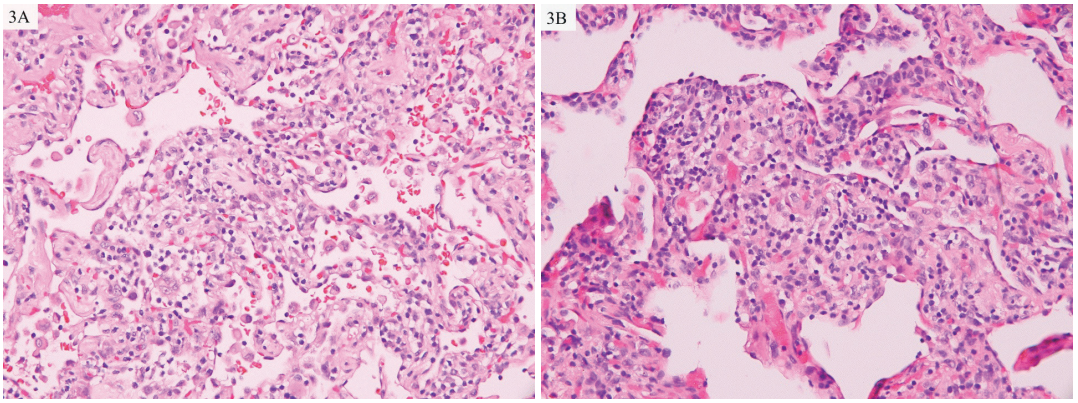

Fig. 3. A. Video-assisted thoracoscopic biopsy revealed cellular chronic interstitial pneumonia (hematoxylin-eosin, original magnification x100); B. Loosely formed granuloma with multinucleated giant cells (hematoxylin-eosin, original magnification x100).

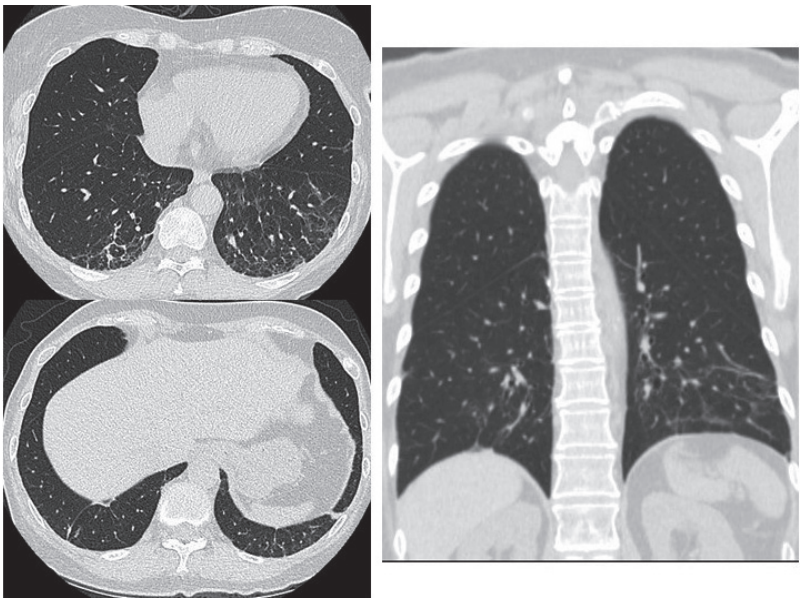

Fig. 4. Follow-up HRCT 4 months later revealed significant resolution of the previous lung lesions.

tered at an initial dose of 10 mg per day. Her symptoms subsided and her breathing sounds became clear. The follow-up pulmonary function test and HRCT were also significantly improved (Table 1, Figure 4). The total duration of steroid therapy was 3 months, and the patient is currently asymptomatic.

Discussion

In this report, we described a steroid-responsive patient with atypical manifestations of CHP with lower lung fibrotic change and neutrophilia in the BAL fluid. This case may provide insight into the challenges in reaching a diagnosis and prognosis of CHP based on current practice.

In general, the BAL features of hypersensitivity pneumonitis consist of high numbers of lymphocytes with a CD8+ T cell predominance [3, 6, 8-11]. In this patient, the lymphocyte counts in the BAL fluid were low, which has been reported previously and might result from the chronicity of the disease course. Ohtani and colleagues first reported a patient with bird fancier's lung disease whose disease progressed from acute to chronic because of persistent antigen exposure. The BAL lymphocyte counts significantly decreased throughout the 4-year follow-up (50% to 27.1%) [12]. Adams and colleagues also found that there were lower lymphocyte counts of total cellularity in fibrotic-type hypersensitivity pneumonitis [11].

However, the abundant neutrophils in the BAL fluid cellularity that we found in our patient are uncommon in CHP in the absence of active pulmonary infections. A possible explanation is that the patient still had intermittent exposure to the offending antigen, which causes an acute inflammatory response, even in the chronic phase of hypersensitivity pneumonitis [13]. Caillaud and colleagues found that among 41 patients with CHP, the shorter the time lapse from antigen exposure, the greater the total cell count and the greater the percentage of neutrophils [5]. Inoue et al studied 19 patients

with bird-related hypersensitivity pneumonitis and found an increased proportion of BAL neutrophils, similar to this report. And, there were concomitant findings of significant elevations of G-CSF, IL-6, IL-8, IL-17 and CXCL-2 in the BAL fluid and serum. An increase in serum TNF-α and IL-10 were also noticed in their study. It can be concluded that neutrophil and Th1 responses would take place in the early phase of recurrent antigen exposure in CHP [14]. This is well correlated with the intermittent symptoms attack in the chronicity of the disease course of this patient. Furthermore, this may also explain why there was a good therapeutic response only to low-dose steroids in this patient.

The HRCT of this patient revealed multiple subpleural patches and focal bronchiectasis in the bilateral lower lungs. It was difficult to differentiate between CHP and idiopathic pulmonary fibrosis (IPF) purely from the image studies for this patient. In fact, the discrepancy between a pathology report and a multidisciplinary discussion is fairly common, especially when atypical features occur (presence of strong autoimmune features, a low lymphocyte level in the BAL fluid, and the lack of a nodular shadow or mosaic attenuation on HRCT) [15]. Table 2 summarizes the differences between CHP and IPF. It is worth mentioning that the presence of traction bronchiectasis or a honeycomb appearance are not uncommon. In the

Table 2. Summary of the Differences between CHP and IPF [2,3,6,9,10,13,16,17,18,19]

	CHP	IPF
Age at diagnosis (years)	Any	> 50
Gender	Female = male	Predominantly male
Bronchoalveolar lavage cellularity (lymph %)	40-50%	7-13%
HRCT features	• Often middle or upper lung zone predominance • Mosaic attenuation (air trapping) • Centrilobular nodules • Mixed reticular and ground glass opacity	• Honeycombing with/without traction bronchiectasis • Reticular abnormality • Subpleural basal predominance
Histopathological features	• Airway-centered interstitial fibrosis • Chronic bronchiolocentric inflammation • Poorly formed non-necrotizing granuloma	• Dense fibrosis with architectural distortion Fibroblast foci
Approved therapies	• Avoid antigen exposure • Immunosuppression • Nintedanib (by US FDA for progressive fibrosing phenotype)[20]	Nintedanib and pirfenidone
Survival	• Varies (nonfibrotic >fibrotic CHP)	• 2-5 years 3.8 years in US (>65y/o)

study by Silva *et al*, most patients with CHP had traction bronchiectasis or traction bronchiolectasis [7]. Similar results were reported by Walsh and colleagues, and the severity of traction bronchiectasis was even associated with increased mortality [16].

Differentiating CHP from IPF is a diagnostic challenge, and a combination of exposure history and even lung biopsy may be needed for accurate results in some cases [2, 3, 7, 11, 17]. HRCT findings were also found to correlate with survival among chronic hypersensitivity patients. In general, those without the presence of fibrosis (mosaic attenuation, air-trapping) have a longer survival than those with fibrosis (honeycombing, traction bronchiectasis, reticulation) (>7.95 vs 2.76) [16, 18, 19]. The good therapeutic response to low-dose steroid in our patient may be explained by the minimal fibrotic change on HRCT and the lack of honeycombing on lung biopsy.

In conclusion, this case report demonstrates that in patients with CHP, recurrent exposure to the causative antigen may induce transient neutrophilic alveolar inflammation. Differentiating between CHP and IPF is a challenge. It is prudent to combine exposure history with histopathology for a definite diagnosis of CHP. Finally, non-fibrotic CHP has a better prognosis than fibrotic CHP, and the less fibrotic change there is, the better the response to anti-inflammatory treatment.

References

1. Sink JN, Ortega HG, Reynolds HY, *et al*: Needs and opportunities for research in hypersensitivity pneumonitis. Am J Respir Crit Care Med 2005; 171(7): 792-8.
2. Lacasse Y, Girard M, Cormier Y: Recent advances in hypersensitivity pneumonitis. Chest 2012; 142(1): 208-17.
3. Spagnolo P, Rossi G, Cavazza A, *et al*: Hypersensitivity pneumonitis: a comprehensive review. J Investig Allergol Clin Immunol 2015; 25(4): 237-50; quiz follow 50.
4. Glazer CS: Chronic hypersensitivity pneumonitis: important considerations in the work-up of this fibrotic lung disease. Curr Opin Pulm Med 2015; 21(2): 171-7.
5. Caillaud DM, Vergnon JM, Madroszyk A, *et al*: Bronchoalveolar lavage in hypersensitivity pneumonitis: a series of 139 patients. Inflamm Allergy Drug Targets 2012; 11(1): 15-9.
6. Adderley N, Humphreys CJ, Barnes H, *et al*: Bronchoalveolar lavage fluid lymphocytosis in chronic hypersensitivity pneumonitis: a systematic review and meta-analysis. Eur Respir J 2020.
7. Silva CI, Muller NL, Lynch DA, *et al*: Chronic hypersensitivity pneumonitis: differentiation from idiopathic pulmonary fibrosis and nonspecific interstitial pneumonia by using thin-section CT. Radiology 2008; 246(1): 288-97.
8. Yoshizawa Y, Ohtani Y, Hayakawa H, *et al*: Chronic hypersensitivity pneumonitis in Japan: a nationwide epidemiologic survey. J Allergy Clin Immunol 1999; 103(2 Pt 1): 315-20.
9. Morisset J, Johannson KA, Jones KD, *et al*: Identification of diagnostic criteria for chronic hypersensitivity pneumonitis: an international modified Delphi survey. Am J Respir Crit Care Med 2018; 197(8): 1036-44.
10. Salisbury ML, Myers JL, Belloli EA, *et al*: Diagnosis and treatment of fibrotic hypersensitivity pneumonia. Where we stand and where we need to go. Am J Respir Crit Care Med 2017; 196(6): 690-9.
11. Adams TN, Newton CA, Batra K, *et al*: Utility of bronchoalveolar lavage and transbronchial biopsy in patients with hypersensitivity pneumonitis. Lung 2018; 196(5): 617-22.
12. Ohtani Y, Hisauchi K, Sumi Y, *et al*: Sequential changes in bronchoalveolar lavage cells and cytokines in a patient progressing from acute to chronic bird fancier's lung disease. Intern Med 1999; 38(11):896-9.
13. Morell F, Roger A, Reyes L, *et al*: Bird fancier's lung: a series of 86 patients. Medicine (Baltimore) 2008; 87(2): 110-30.
14. Inoue Y, Ishizuka M, Furusawa H, *et al*: Acute inflammatory and immunologic responses against antigen in chronic bird-related hypersensitivity pneumonitis.

Allergol Int 2019; 68(3): 321-8.
15. Zaizen Y, Tabata K, Yamano Y, *et al*: Histology is critical but not always for the diagnosis of chronic hypersensitivity pneumonitis. Respir Investig 2020.
16. Walsh SL, Sverzellati N, Devaraj A, *et al*: Chronic hypersensitivity pneumonitis: high resolution computed tomography patterns and pulmonary function indices as prognostic determinants. Eur Radiol 2012; 22(8): 1672-9.
17. Chung JH, Montner SM, Adegunsoye A, *et al*: CT findings associated with survival in chronic hypersensitivity pneumonitis. Eur Radiol 2017; 27(12): 5127-35.
18. Salisbury ML, Gu T, Murray S, *et al*: Hypersensitivity pneumonitis: radiologic phenotypes are associated with distinct survival time and pulmonary function trajectory. Chest 2019; 155(4): 699-711.
19. Chung JH, Zhan X, Cao M, *et al*: Presence of air trapping and mosaic attenuation on chest computed tomography predicts survival in chronic hypersensitivity pneumonitis. Ann Am Thorac Soc 2017; 14(10): 1533-8.
20. Flaherty KR, Wells AU, Cottin V, *et al*: Nintedanib in progressive fibrosing interstitial lung diseases. N Engl J Med 2019; 381(18): 1718-27.